

# **Fully Automated Tumor Segmentation from Ultrasound Images by Choosing Dynamic Thresholding**

by

A Thesis Presented to the Academic Faculty

**Md. Musfiqul Islam (170021007)**

**Md. Tawsif Mostafiz (170021031)**

**Seemab-Al-Mujaddeed (170021041)**

A Thesis Submitted to the Academic Faculty in Partial Fulfillment of the  
Requirements for the Degree of

**BACHELOR OF SCIENCE IN ELECTRICAL AND ELECTRONIC  
ENGINEERING**



Department of Electrical and Electronic Engineering

**Islamic University of Technology (IUT)**

Gazipur, Bangladesh

May 2022

A dissertation on  
**Fully Automated Tumor Segmentation from Ultrasound Images by  
Choosing Dynamic Thresholding**

Approved by:



.....

**Dr. Md. Taslim Reza**

Professor, Department of EEE

Islamic University of Technology (IUT),

Gazipur-1704, Bangladesh.

Date: 16.05.2022  
.....

## Declaration of Authorship

This is to certify that the work given in this thesis paper is the result of the study accomplished by the students under the supervision of Prof. Dr. Md. Taslim Reza, Islamic University of Technology's Department of Electrical and Electronic Engineering (EEE) (IUT). It is further claimed that no part of this thesis paper has been submitted anywhere else for the purpose of receiving a degree or a presumption.

### Authors

*M. Islam*

---

Md. Musfiqul Islam

ID- 170021007

*T. Mostafiz*

---

Md. Tawsif Mostafiz

ID- 170021031

*Seemab-Al-Mujaddeed*

---

Seemab-Al-Mujaddeed

ID-170021041

# TABLE OF CONTENTS

List of Figures.....	v
List of Tables.....	viii
List of Abbreviation.....	xi
Abstract.....	xiii
<b>Chapter 1. Introduction.....</b>	<b>1</b>
1.1 Introduction.....	1
1.2 The Impact of This Study.....	2
1.3 Objectives of this Research.....	3
1.4 Main Contributions.....	3
1.5 Thesis Overview.....	4
<b>Chapter 2. Literature Review.....</b>	<b>5</b>
2.1 Introduction to Ultrasound Imaging.....	5
2.1.1 Various applications of ultrasound imaging .....	7
2.2 Methods used in Algorithm.....	15
2.3 Precision Matrices.....	18
2.4 Relevant Research.....	20
<b>Chapter 3. Methodology.....</b>	<b>22</b>
3.1 Introduction.....	22

3.2 Data collection.....	23
3.3 Types of Images.....	24
3.4 How the algorithm works.....	25
<b>Chapter 4. Results and Discussion.....</b>	<b>29</b>
4.1 Introduction.....	29
4.2 Results for data samples.....	29
4.3 Final Result.....	36
4.4 Discussion.....	36
<b>Chapter 5. CONCLUSION.....</b>	<b>37</b>
5.1 Introduction.....	37
5.2 Future scopes of Research.....	37
5.3 Conclusion.....	38
References.....	39
Appendix A.....	43

## LIST OF FIGURES

Sl. No.	Fig. No.	Name of the Figure	Page No.
01	2.1	Image of a transducer used in an ultrasound process	5
02	2.2	(a) Medical ultrasound transducer with a single matching layer and backing block (b) In Ultrasound transducer for flaw detection graphite is used for the purpose of pairing and t	6
03	2.3	Sound wave trough Auditory Canal. Reprinted from “Roshni's Physics E-Portfolio	7
04	2.4	(a) Medical ultrasound transducer with a single matching layer and backing block (b) Ultrasound transducer for flaw detection uses graphite for matching and wear resistance	8
05	2.5	A piezoelectric crystal is inserted between a solid base and the impulse accumulating part in a standard piezoelectric transducer, as shown in the diagram.	8
06	2.6	Ultrasound interaction with tissues Mechanism	11
07	2.7	(a) Attenuation of Ultrasound waves, (b) Depth and time, (c) Impedance difference and echo intensity	14
08	2.8	Two types of Dynamic Thresholding (a) Local pixel-wise unilateral learning-based method (b) Global parametric bilateral ratio-based method	15

<b>Sl. No.</b>	<b>Fig. No.</b>	<b>Name of the Figure</b>	<b>Page No.</b>
09	2.9	Thresholding method implementation in MATLAB	15
10	2.10	Image segmentation with a Watershed algorithm	16
11	2.11	Watershed algorithm implementation in MATLAB	16
12	2.12	Chan-Vese model for active contours implementation in MATLAB	17
13	2.13	SRG method implementation on MATLAB	18
14	2.14	Jaccard similarity coefficient for set A and set B	19
15	2.15	Uses of Jaccard similarity index/Jaccard index for ‘single-cell cluster’ stability using the Jaccard similarity index.	19
13	3.1	Our proposed algorithm flowchart	22
14	3.2	Samples of Ultrasound breast images dataset	23
15	3.3	For finding the threshold value while segmented area has a large B&W pixelratio 1	25
16	3.4	For finding the threshold value while segmented area has a large B&W pixelratio 2	26
17	3.5	Segmented Image from dataset-1 (us110.bmp) in Matlab implementation	26
18	3.6	Active Contour requires a ROI for segmentation.	27
19	3.7	Shadow is removed using Matlab implementation	28

<b>Sl. No.</b>	<b>Fig. No.</b>	<b>Name of the Figure</b>	<b>Page No.</b>
20	3.8	Watershed- Active Contour Model applied to the shadow removed images	28
21	3.9	Image without Shadow (us159.bmp)	29
22	3.10	Image where no Shadow (us117.bmp)	30
23	3.11	Image Without Shadow (us112.bmp)	30
24	3.12	Image Without Shadow (us161.bmp)	31
25	3.13	Image Without Shadow (us159.bmp)	31
26	3.14	Image With Shadow Elimination (us90.bmp)	32
27	3.15	Image With Shadow Elimination (us45.bmp)	32
28	3.16	Image Without Shadow ( malignant(1).png )	33
29	3.17	Image Without shadow ( benign(49).png )	33
30	3.18	Image With Shadow Elimination ( benign(103).png )	34
31	3.19	Image With Shadow Elimination ( benign(190).png )	34
32	3.20	Image With Shadow Elimination ( benign(103).png )	35
33	3.21	Image With Shadow Elimination ( benign(10).png )	35



## LIST OF TABLES

Table 2.1 The amount of photos in each of the three kinds of breast tumors.....	09
Table 4.1: final result of our study.....	36

*Dedicated*

To

*Our beloved parents, whose constant support and guidance  
made it all possible for us*

## ACKNOWLEDGEMENTS

Every journey comes to an end, and ours is no different. It had been almost a year and a half since we started working on our project, and since then it had been such an integral part of our academic life that concluding this book feels like letting go of a part of ourselves. When we started our research in the chilly winter of 2020, we had been driven by a hope to make a difference on the ever-building mass of human knowledge, to improve upon what has already been done, and even dared to build something unique. It is not our place to say if we have been successful in our endeavor or not, neither do we wish to. At the end of the road, we just want to thank those who were our guides along this eventful journey.

First, we would like to thank our respected thesis supervisor, Professor Dr. Taslim Reza for his ever-gracious support. We had made mistakes, and more than once felt like we were stuck at a dead end. But we could always rely upon his kind encouragement and valuable insights to put us on the right path. We consciously admit that we have not always been as earnest in our effort as we should have been, but Sir had been patient with us, and without his support, this journey would have been impossible.

Secondly, we want to thank those researchers in this field, whose work provided us with the facts and data that had been the building blocks of our project. We have not started from nothing, and our idea has been the summation of all the hard-working individuals around the world who are continuously working to the advancement of the human race, striving to surpass what had been deemed impossible in the past. We owe our highest gratitude to these people of science.

Thirdly, our journey started in accordance with our department's academic policy. It had been the ignition at the inception of our research that allowed us to start working on our thesis and seek guidance from our respected supervisor. We had the opportunity to give two different presentations on the state of our thesis among the respected faculties and each provided us with opportunities to find our flaws and finesse our project even further.

And finally, all praise goes to Allah, the Almighty and merciful. We understand that the fact that we have been able to finish this thesis so gracefully and found help and counsel whenever we most needed it had been Allah's kindness upon us. We only hope that Allah continues to guide us in our future journeys so that we can work for the betterment of humanity.

## LIST OF ABBREVIATIONS

<b>BUS</b>	Ultrasound image
<b>SHM</b>	Simple Harmonic Motion
<b>RF</b>	Radio Frequency
<b>PRF</b>	Pulse Repetition Frequency
<b>TGC</b>	Time Gain Compensation
<b>ROI</b>	Region-of-Interest
<b>KNN</b>	K Nearest Neighbors
<b>SRG</b>	Seeded Region Growing

## **ABSTRACT**

The main fortitude of diagnostic ultrasound are its ability to reveal the mechanical composition of anatomy, the dynamic mobility of organs and instant details of blood circulation. Breast ultrasound imaging is congenital, radiation-free, and convenient. Automatic breast ultrasound (BUS) image segmentation is difficult in clinical practice but vital for cancer diagnosis and medication planning. Speckle noises and attenuated artifacts are prominent in ultrasound images. Speckles obscure aspects that are essential for diagnosis and evaluation. Due to low contrast, automatically finding areas of interest (ROIs) and inaccurate tumor boundaries in breast ultrasound images (BUS), automatically segmenting breast tumors from ultrasound remains a challenge. The majority of ultrasound image segmentation algorithms are centered on region growing or active contours. These are semi-automatic segmenting methods in which seed points or preliminary contours have to be identified manually. This thesis presents a fully automated tumor segmentation from Ultrasound Images by choosing dynamic thresholding. This framework also includes selection of an automated threshold value for watershed method. The area and boundary error metrics are used to evaluate the performance of the proposed completely automatic segmentation method on a BUS database. Our proposed method is more accurate and reliable in the segmentation of BUS images than the fully automated method recently proposed.

# Chapter 1

## INTRODUCTION

### 1.1 Introduction

Among women breast cancer is the most diagnosed malignant disease [1, 2]. In 2016, about 246,660 women were diagnosed with breast cancer which is considered as the highest level of 29% among other kinds of cancers [3]. For the expected deaths, breast cancer is the second highest in women which alone accounts 14% against other cancer types [3]. Breast cancer outcomes lead to increasing with early detection. Breast ultrasound (BUS) is a prominent imaging modality for early detection and diagnosis of breast cancer. However, clinical experience and expert knowledge are necessary to achieve correct diagnosis [4]. “Segmentation is a critical step in a BUS CAD system.” Manual Segmentation methods are time- consuming and tedious and suffer from great individual variability [5].

As a traditional medical imaging tool, Ultrasound (US) has played a significant part in breast cancer detection. Breast US images can enhance mammography via identifying breast malignancies that are not apparent on a typical mammogram. Dissipation, shadowing, speckle, and signal dropout are common artifacts that hamper the segmentation process; However, to the orientation dependence of acquisition, something may result in missing edges. By integrating area, threshold, portability, transducer design and various thicknesses to cope with the intrinsic artifacts present in US images, a fully automatic technique for segmenting tumor area for traditional B-mode US images has been developed.

Breast tumors can be classified qualitatively and quantitatively using contrast- enhanced ultrasound imaging. Ultrasound contrast agents primarily act as nonlinear scatters due to variations in wave propagation and elastic modulus between microbubbles and surrounding area. In this sense after enhancement patterns, various perfusion phases can be characterized. Another is volumetric echo, where a matrix array detection process is being used. Replacing a single row of elements in conventional linear transducers, the elements in a matrix array transducer are arranged in a 2-D grid.

Matrix array generates a beam in both positions, thus forming an entire, pyramid-shaped volume [6]. In our approach, thresholding is applied to generate a binary image from a grayscale image where the threshold value serves as the contrast ratio (0-1). Thresholding methods depend on the intensity and how each pixel in an image replaces with black pixel. To fully automate thresholding, the computer must automatically assign the threshold (T). Contiguous zones of interest can be segmented into different objects using the watershed method. By treating an image as a surface area with light pixels representing high elevations and dark pixels representing low elevations, the watershed method helps to find "catchment basins" or "watershed ridge lines" in the image. Chan-Vese model is one of the most used segmentation methods [7] which can be used to segment several types of images and used in images that are difficult with other methods. It is based on the Mumford-Shah functional [2] for segmentation and is a commonly used technique in the medical imaging field, mostly for the segmentation of the brain, heart, and breast tissues [8]. When seed-based region growing method is used to determine the overall segmentation it is especially important to select an initial seed. In the last phase, we also differentiate the images into two formations- Image with Shadow region and Image with No Shadow region. Afterward, the input signal of each region of interest is computed, and the necessary parameters and values for tumor identification are extracted. Because we are measuring our detection accuracy with three precision matrices (Dice score, BF score, Jaccard Index). The harmonic average (F1 measure) of classifier value performance is used in conjunction with distance error tolerance to determine if a point on the anticipated boundary matches the ground truth boundary with respect to BF score. We have detected more accuracy in the field of comparison set of predicted labels for a sample to the corresponding set of labels via Jaccard index values. We create an automated system to label a ground truth region in your image. The Dice score, which really is a measure of how similar objects are, is used to validate our algorithm.

## 1.2 The impact of this study

Early detection is the main key respect to the field on Breast tumor. The main purpose of breast cancer screening tests is to discover abnormalities in the breast as early as feasible. Breast cancer was diagnosed in approximately 246,660 women in 2016, representing the highest rate of 29 percent among all tumors [3]. Breast cancer is the second leading cause of anticipated death in women, accounting for 14% of all cancer fatalities [3]. Breast cancer outcomes lead to increasing with early detection. Breast ultrasound (BUS) is a prominent imaging modality for early detection and diagnosis of breast cancer. In Bangladesh, the occurrence of breast cancer is estimated to be about 22.5 per



100000 females of all ages, and breast cancer has the highest prevalence of 19.3 per 100000 compared to any other cancer for Bangladeshi women aged 15-44 years [9]. In the United States, studies indicate breast cancer as the most-commonly detected cancer, as well for women [10]. One in every eight women are affected by breast cancer in the period spanning from birth till death. There is expected to be 268,600 new cases of invasive breast cancer in America in 2019 alone, amongst which 41,760 deaths are expected [11]. As an outcome, there is a renewed interest in learning how to apply one of the oldest image processing techniques, image segmentation, to ultrasound data in BUS image detection. Our process signifies the fastest and highly accurate process to detect the breast tumor. Thus, it is extremely helpful for recovery from tumor. A robust process programmed in MATLAB code in this regard.

### 1.3 Objectives of this research

The following are the primary objectives as we want to create an algorithm that can:

- I. Early detection is the key.
- II. Perform tumor segmentation fully automatically without any user intervention.
- III. Selects an automated threshold value for Watershed Method.

### 1.4 Main Contributions

Our main contribution in this thesis as the objectives of the research described earlier is as follows:

As we are measuring our detection accuracy with three precision matrices (Dice score, BF score, Jaccard Index)

- We have detected more accuracy in the field of comparison set of predicted labels for a sample to the corresponding set of labels via Jaccard index values.
- To assess if a point on the predicted boundary matches the ground truth boundary with regard to BF score, the harmonic mean (F1-measure) of the performance of the classifier parameters is employed in conjunction with a distance error tolerance.
- We create an automated system to label a ground truth region in your image. The Dice score, which really is a measure of how similar objects are, is used to validate our algorithm.

## 1.5 Thesis Overview

As our thesis work mentions above, here is our overview of our outcome as follows:

Basically, Chapter 1 is expected to provide background and goal orientation for this research, as well as the purpose of the research, the research's primary contributions, and the goals it intended to obtain.

Chapter 2 examines the literature on statistical ultrasound methods, as well as the conceptual components of current research.

Chapter 3 discusses the suggested algorithm used in this study, as well as the procedures and techniques used to extract the parameters used to distinguish between benign and malignant breast cancers, as well as images with or without shadows.

Chapter 4 focuses on the research's simulations and categorization outcomes, as well as the impact of multiple parameters on the study's outcome, which is called one step ahead for the detection of breast tumors.

The work is summarized and conclude in Chapter 5 with a perspective of future research directions in this field.

## Chapter 2

### Literature Review

#### 2.1 Introduction to ultrasound imaging

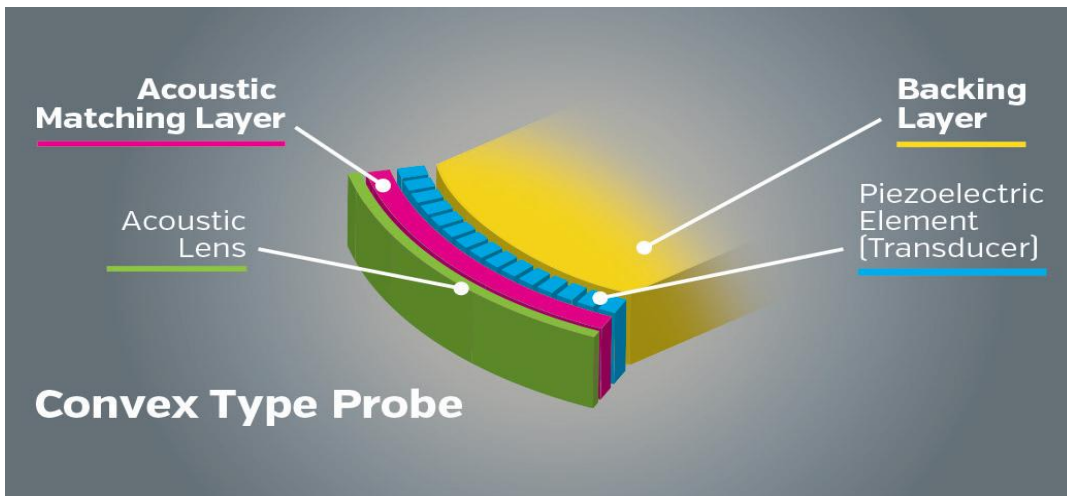
Ultrasound was first evolved as SONAR (Sound Navigation and Ranging) technology to detect submarines during World War I. High-frequency sound waves are used in ultrasound imaging (mammography) to observe inside the organ. In the 1950s, ultrasound was first employed in medicine, with early applications in gestational sonography. But in recent past, Ultrasound usage in medical perspectives have been increased widely. Especially Ultrasound Imaging in the field of Biomedical sectors.

Because ultrasound images are collected instantaneously, they can show internal organ mobility as well as blood circulating along blood vessels. Ultrasound imaging does not expose anyone to ionizing radiation like X-ray imaging does.

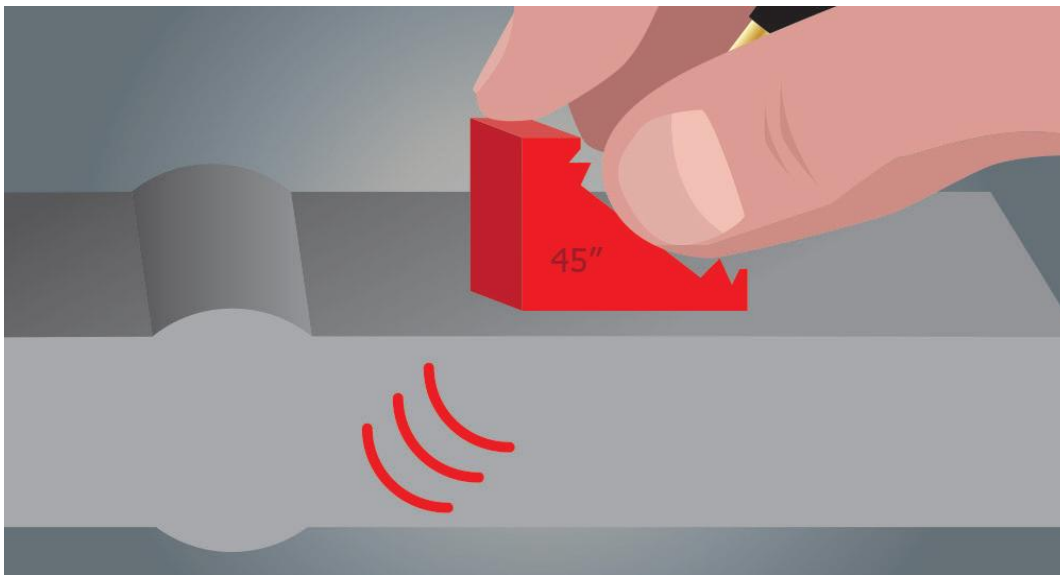
In an ultrasound, a converter is applied to the skin or inserted into a bodily orifice. The ultrasounds are delivered from the transducer into the body through a small layer of gel placed to the skin.



Fig 2.1: Usage of Transducer while experimenting a Ultrasonography. Reprinted from “Diagnostics of pregnancy Pregnant woman getting ultrasound from doctor Ultrasound Stock Photo [35]



(a)



(b)

Fig 2.2: (a) Medical ultrasound transducer with a single matching layer and backing block ; (b) Ultrasound transducer for flaw detection uses graphite for matching and wear resistance; [39] .

US image is created by sending sound waves in body tissues, and capturing the reflections, based on the amplitude of the wave, and the time it takes for the wave to come back [12].

### 2.1.1 Various applications Ultrasound imaging

Ultrasound imaging can help a physician evaluate medical conditions more precisely and treat more efficiently. There are multiple methods for ultrasound imaging. Common ultrasound imaging procedures include:

- (a) Intestinal ultrasound (to envisage abdominal organs and tissues)
- (b) Breast ultrasound (to envisage breast tissue)
- (c) Doppler fetal heart rate screen (to heed to the embryonic heartbeat)
- (d) Bone sonometric (to check for bone density)
- (e) Doppler ultrasound (seeing the flow of blood through some kind of blood channel, organ or other entities)
- (f) Ophthalmic ultrasound (to make ocular features visible)
- (g) Electrocardiogram (to examine the heart)
- (h) Fetal ultrasound (seeing a fetus during pregnancy)
- (i) Ultrasound-guided biopsies (for collecting a sample of tissue)

Ultrasound imaging is all about Sound Wave. Sound is a wave formed by oscillating objects and moved across a medium via particle interaction from one region to another (Fig. 2.3). These molecules vibrate longitudinally, in a parallel direction to the wave's direction. Ultrasound is created by sound waves with frequency greater than 20,000 Hz. It is inaudible to the human ear because it occurs at frequencies outside the range of human hearing.

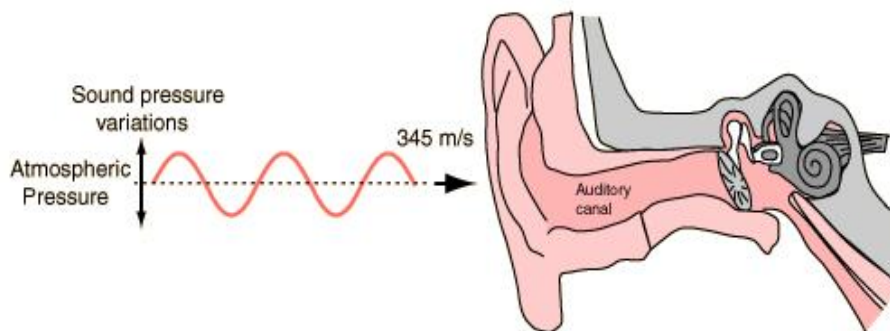


Fig 2.3: Sound wave trough Auditory Canal. Reprinted from “Roshni's Physics E-Portfolio [36]”

A sound wave is composed of a number of periodic oscillations of particles in a medium. These cycles generate compression and re-polarization regions all across the medium.

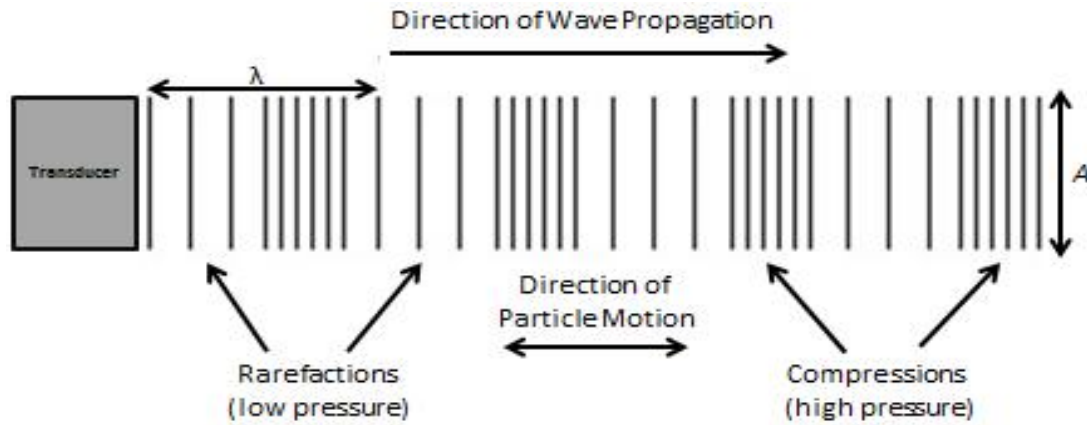


Fig 2.4: Direction of sound wave while propagating. Reprinted from “Roshni's Physics E-Portfolio [36]”

To understand the propagation of sound waves, we imagine a slinky moving down a staircase. If it is going downwards, the Slinky's motion begins by expanding. As the first ring expands forward, it pulls the rings behind it forward, causing a compression wave. This push and pull chain reaction causes each ring of the Slinky's coil to be displaced from their original location, gradually transporting the original energy from the first coil to the last [13].

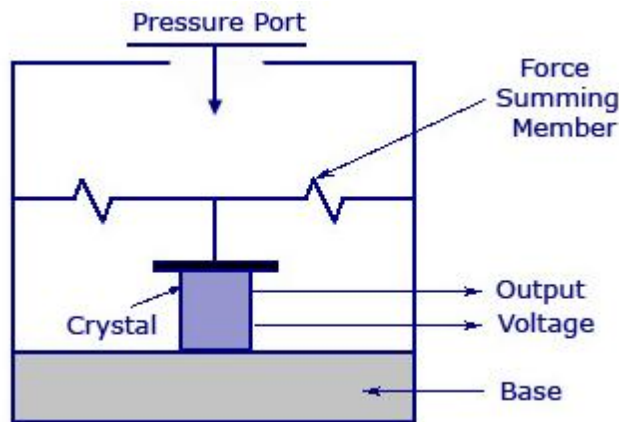
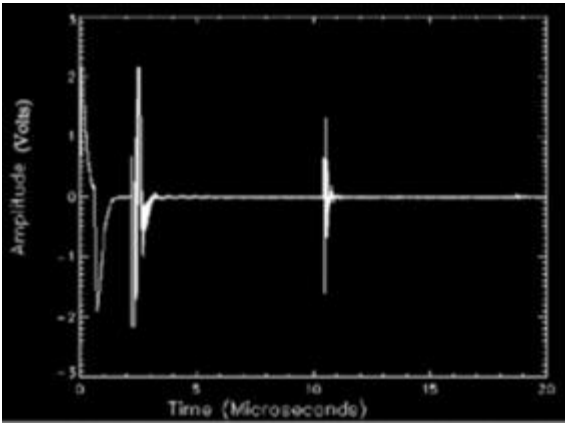

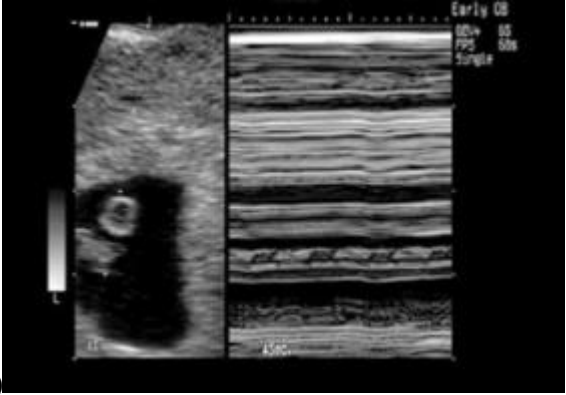


Fig 2.5: A piezoelectric crystal is inserted between a solid base and the impulse accumulating part in a standard piezoelectric transducer, as shown in the diagram

Table 2.1 Different types of ultrasound scan [14]

Type of scan	How echo is received	Example of scan
A mode	Amplitude mode	 <p data-bbox="1036 863 1292 894">Fig: Amplitude mode</p>
	Each layer producing a reflection shows up as a peak on the trace. The larger the echo, the higher the peak	
B mode	Brightness mode	 <p data-bbox="1003 1440 1325 1472">Fig: Musculoskeletal detail</p>
	Each reflecting echo is registered as a bright spot; the larger the amplitude of the reflecting echoes, the brighter the spots	

M mode	Motion mode	<p>Fetal pole (B mode) + waveform (M mode)</p>  <p>mode)</p>
	Moving echoes are recorded to give traces of fetal heart pulsations	

Because the use of ultrasound in diagnosis, rehabilitation, and surgery expands, it is necessary that we have a complete understanding of the biological impacts of this emission. These studies have emerged as one of the most promising fields of modern intensive research. On however one aspect, sound energy is transferred and the convective heat has an impact on tissue. Ultrasound can also disrupt biological material through ablative mechanisms. Mainly thermal processes, for example, can explain the formation of regional ultrasonic lesions in brain tissue at levels of intensity below 200 Watt/cm. This is shown by considering acoustic absorption, heat diffusion, and thermal sensitivity of brain tissue. On the other hand, non- thermal mechanisms are clearly needed to explain reduction in growth rate, mitotic index and chromosomal aberrations which are observed in plant roots irradiated by ultrasound. Despite extensive applications of ultrasound in diagnosis, therapy and even surgery, there are still many problems to be solved in the basic physics of sound propagation in tissues. Sound absorption occurs primarily at the macro-molecular level. There is evidence to indicate that this absorption can be profoundly modified by macro-molecular interaction. The specific physical or chemical relaxation mechanisms responsible for the absorption are unknown. Macroscopic homogeneity in tissue affect the spread of sound and can lead to artifacts in certain tissue absorption measurement methods. The problem of linearity require investigation [15].



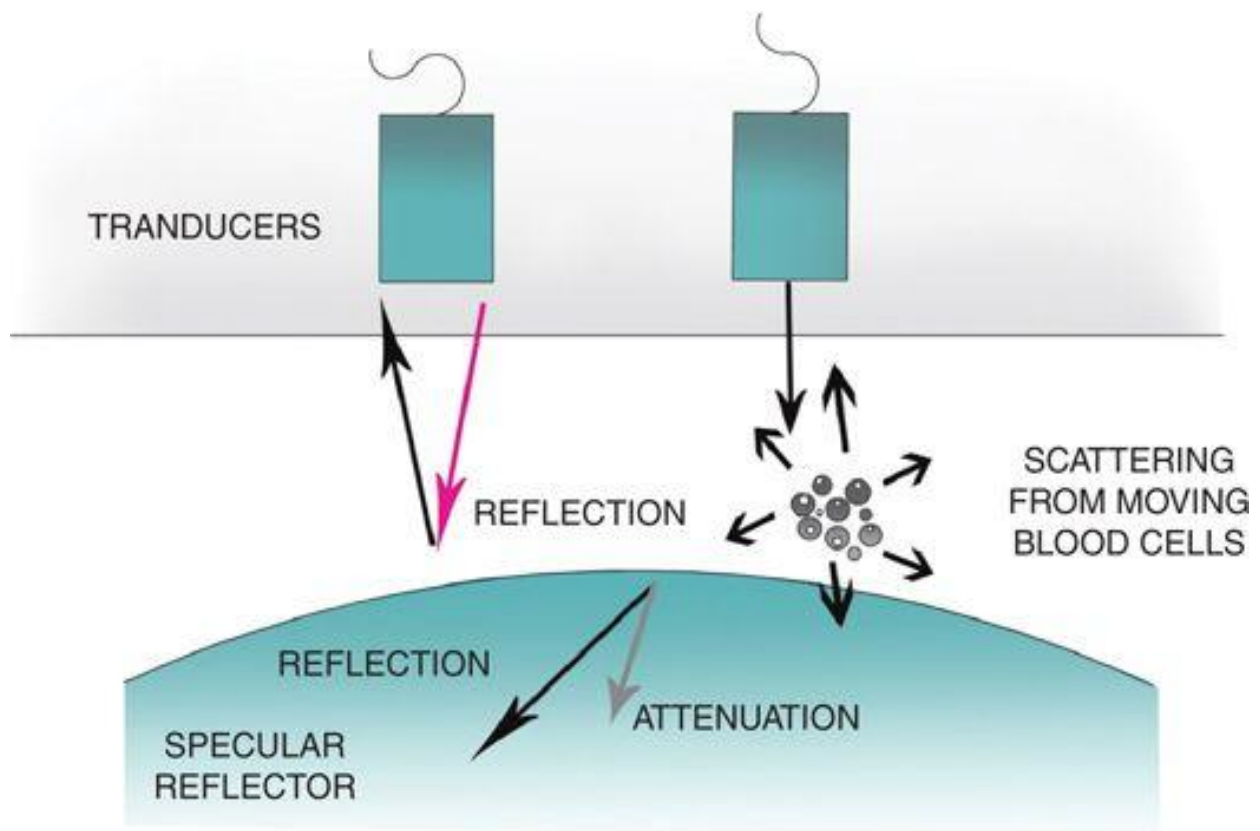


Fig 2.6: Ultrasound interaction with tissues Mechanism. Reprinted from “Fastest Anesthesia & Intensive Care & Emergency Medicine Insight Engine\_ Figure 2.1 [37]”

## Tissue Interactions

When ultrasound waves hit a medium, they cause expansion and compression of medium-term. The interaction between US waves and body tissues occurs in four different manners. Those interactions are:

- Reflection
- Scattering
- Refraction
- Attenuation

## Reflection:

Reflection means when the ultrasound wave strikes a body material, and is deflected towards the transducer.

The main factors that affect reflection are:

- Angle of incidence
- Acoustic impedance mismatch
- Width of the tissue boundary
- Angle of tissue boundary

## Scattering:

Scattering happens when the lateral dimension of the tissue boundary is less than one wavelength of the ultrasound wave propagated. If there are many small tissue boundaries, scattering can radiate in all directions. The signal that reaches the transducer is a much weaker signal than the transmitted signal and is typically 100-1000 (40 - 60 dB) less than the transmitted signal. Most scattering occurs with red blood cells, which have a width of 7-10  $\hat{\mu}\text{m}$ , which is 20 times smaller than the ultrasound wavelength (0.2 to 1 mm (about 0.04 in)). A filter can ignore small signals from red blood cells below a threshold value. Hematocrit has minor impact on Doppler signal.

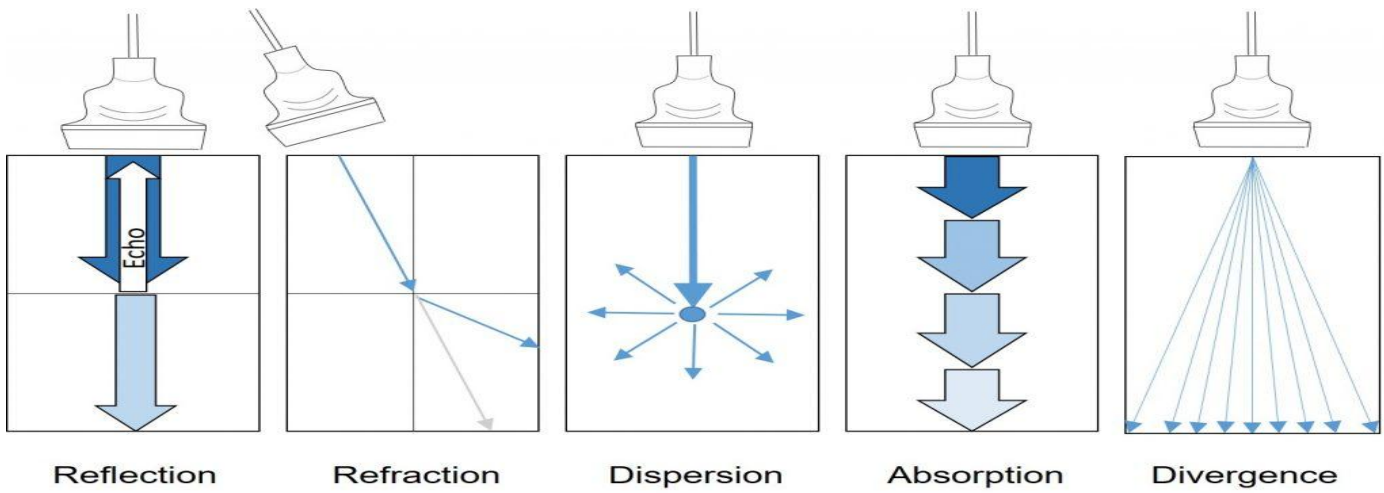
## Refraction:

Refraction occurs when instead of getting back towards the transducer, the wave scatters in a different direction. Ultrasound waves are only refracted at a different medium interface with a different acoustic impedance. Refraction allows improved image quality with acoustic lenses. Refraction can result in ultrasound double-image artifacts.

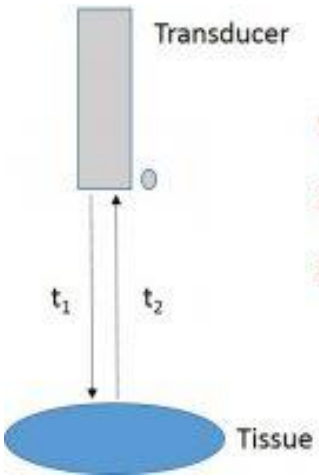
## Attenuation:

Attenuation means reduced amplitude of wavelength. When ultrasound wave travels through a medium, the medium absorbs some of the energy of the ultrasound wave. The amount of energy absorption, or acoustic impedance (Z), defines product of the density of the medium and the propagation velocity of the ultrasound wave." The acoustic impedance formula is shown below: Acoustic Impedance (Z) = Density ( $\rho$ ) x Propagation Velocity (c) (Acoustic impedance formula) During attenuation the ultrasound wave stays on the same path and is not deflected. As it passes through tissues of different densities, the breadth decreases. If all the ultrasound wave energy is absorbed, then structures distal to the point of total attenuation will not be visualized and will appear to be "dropped". This is called dropout. Energy is lost when reflection, scattering and damping occurs. The loss of energy leads to a noisy background. If the SNR is good, a clear image is displayed. A poor SNR eventually leads to a blurred picture. Attenuation is frequency dependent. Low frequencies have better penetration and are therefore not attenuated as much as higher frequencies. In conclusion, the factors that affect attenuation are:

- Transducer Frequency
- Acoustic Impedance
- Acoustic Impedance Mismatch



(a)

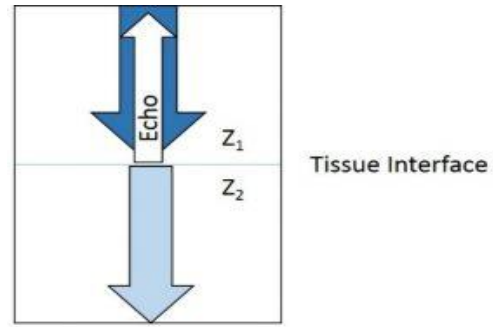


$$\text{Velocity} = \text{Distance} / \text{Time}$$

$$2 \times \text{Depth} = \text{Velocity} \times (t_1 + t_2)$$

$$\text{Depth} = \text{Velocity} \times 0.5 (t_1 + t_2)$$

(b)



$$I_{\text{Echo}} = \left( \frac{Z_1 - Z_2}{Z_1 + Z_2} \right)^2 \times I_0$$

(c)

Fig 2.7: (a) Attenuation of Ultrasound waves, (b) Depth and time and (c) Impedance difference and echo intensity Figure (a),(b) & (c) Reprinted from "Ultrasound Theory Module\_FAMUS [38]"

## 2.2 Methods used in Algorithm

In our research, several methods have been used to make things time consuming and easier and safer for the patients. The methods we have used are as follows:

### Thresholding based Method

Thresholding is a type of segmentation method, where color image is made black and white by eliminating the pixels under the threshold value. We use thresholding to select areas of interest (ROI) of an image, while ignoring the parts we are not concerned with [28]. The threshold value serves as the contrast ratio [0 to 1] in this approach, which converts a grayscale US image to a binary image.

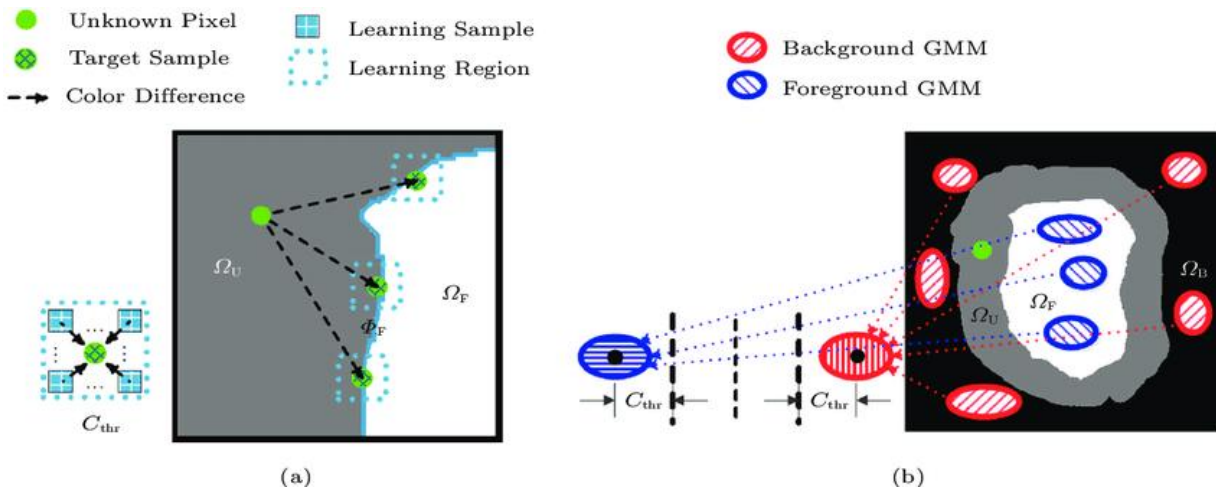


Fig 2.8: Two types of Dynamic Thresholding (a) Local pixel-wise unilateral learning-based method (b) Global parametric bilateral ratio-based method [40].

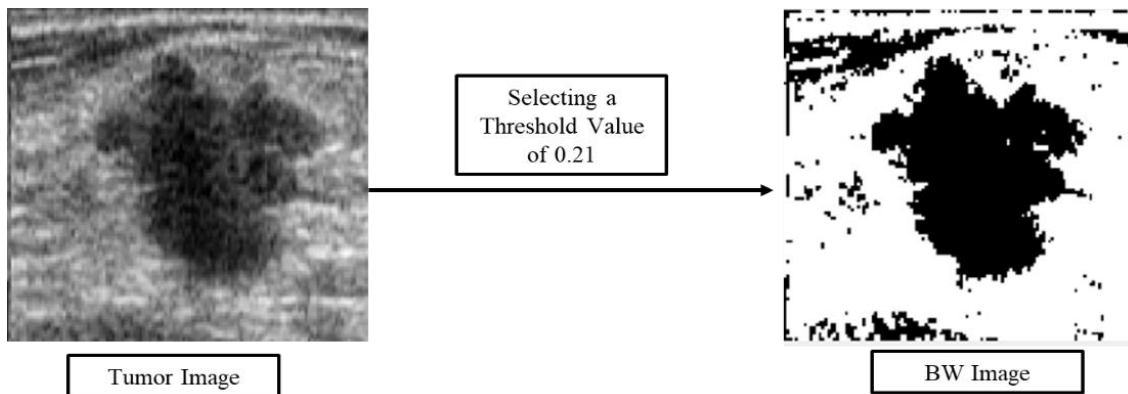


Fig 2.9: Thresholding method implementation in MATLAB

## Watershed Method

The watershed method is used for segmentation in some complex images as if we apply simple thresholding and contour detection then it will not be able to give proper results. Watershed algorithm is based on extracting background and foreground, and then using markers will make watershed run and detect the boundaries. This algorithm helps in detecting touching and overlapping objects in image [29].

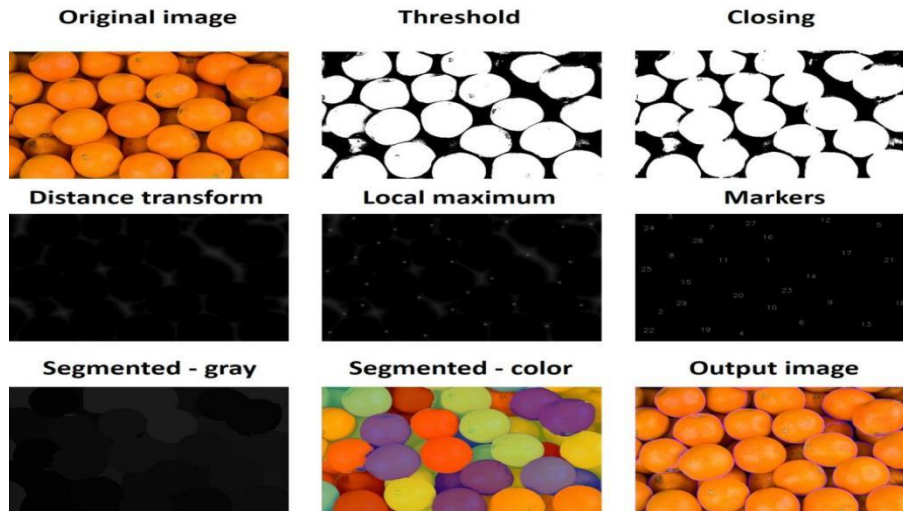


Fig 2.10: Image segmentation with a Watershed algorithm [42]

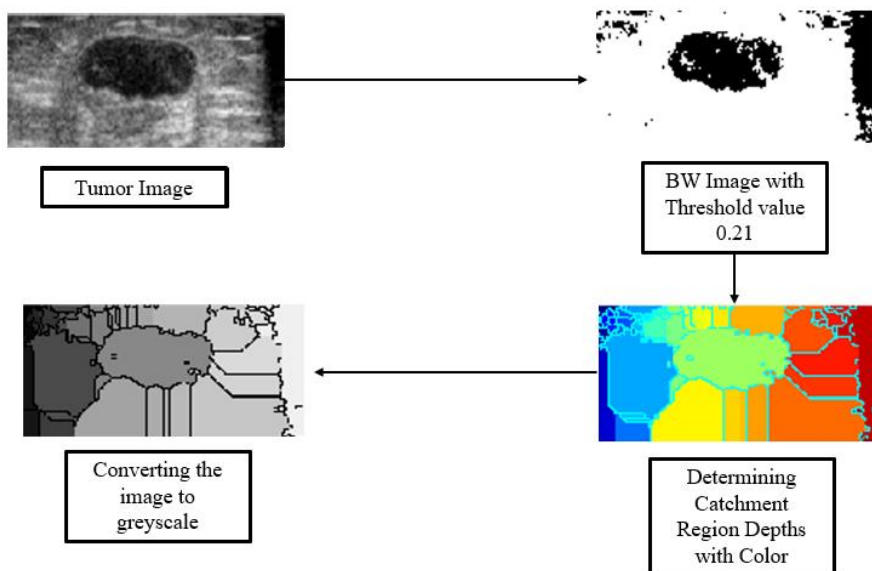


Fig 2.11: Watershed algorithm implementation in MATLAB

## Active Contour Algorithm (Chan-Vese)

Chan-Vese model for active contours [7] is a powerful and flexible method which can segment many types of images, including some that would be quite difficult to segment in means of "classical" segmentation – i.e., using thresholding or gradient based methods.

This model is based on the Mumford-Shah functional [8] for segmentation, and is used widely in the medical imaging field, especially for the segmentation of the brain, heart and trachea [30]. The model is based on an energy minimization issue, which can be reformulated in the level set formulation, leading to an easier way to solve the problem.

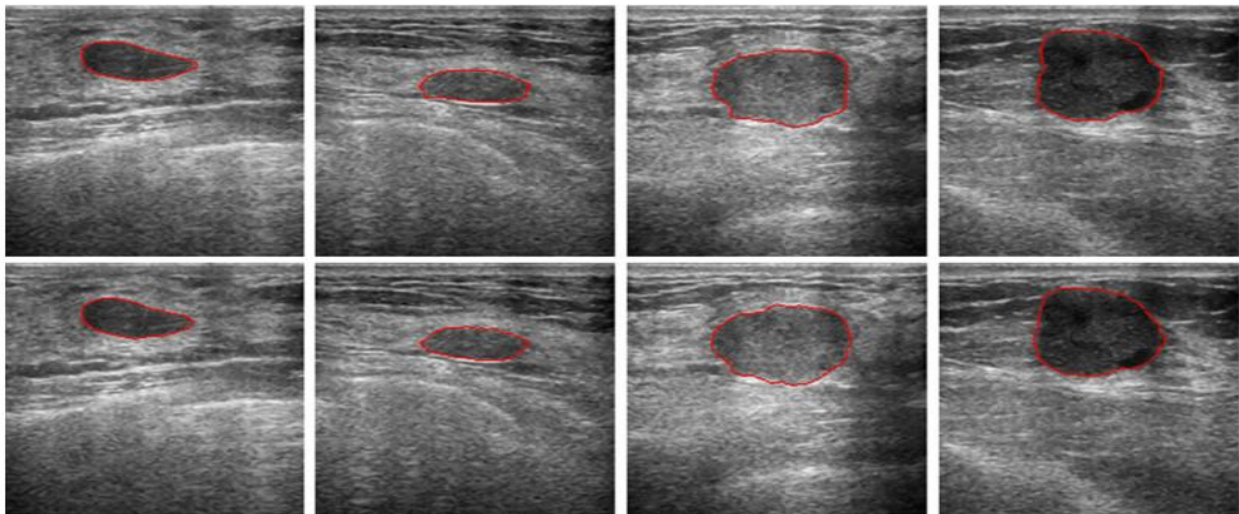


Fig 2.12: Chan-Vese model for active contours implementation in MATLAB

## Seeded Region Growing Method

Seeded region growing (SRG) is another efficient for image segmentation. It begins with a seed point selected by the user where it finds other local similar clusters. SRG then grows these seeds into regions by successively adding neighboring pixels. It finishes when all pixels in the image are assigned to one (and only one) region. The growing strategy of SRG implicitly assumes that pixels from the same region share the same gray value [31].

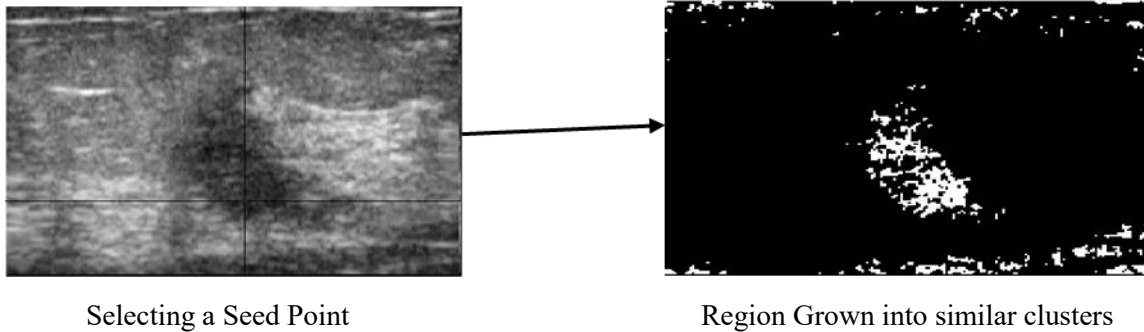


Fig 2.13: SRG method implementation on MATLAB

## 2.3 Precision Matrices

**DICE Score:** The Dice score is a typical indicator for measuring image segmentation algorithms.

The earliest Sørensen's formula was designed for data sets to find the dice score.

$$\text{Dice score} = 2 \times \frac{\text{Area of the Overlap}}{\sum \text{Pixels of both images}}$$

The Dice score, which really is a measure of how similar the objects are, is used to validate our algorithm.

**BF Score:** The harmonic mean (F1-measure) of the performance of the classifier values is used in conjunction with a distance error tolerance to determine if a point on the anticipated boundary matches the ground truth boundary with respect to BF score.

%%Bfscore convention (Contour matching score for image segmentation) in matlab-

#Syntax- score = bfscore(prediction,groundTruth)

[score,precision,recall] = bfscore(prediction,groundTruth)

[\_\_\_] = bfscore(prediction,groundTruth,threshold)

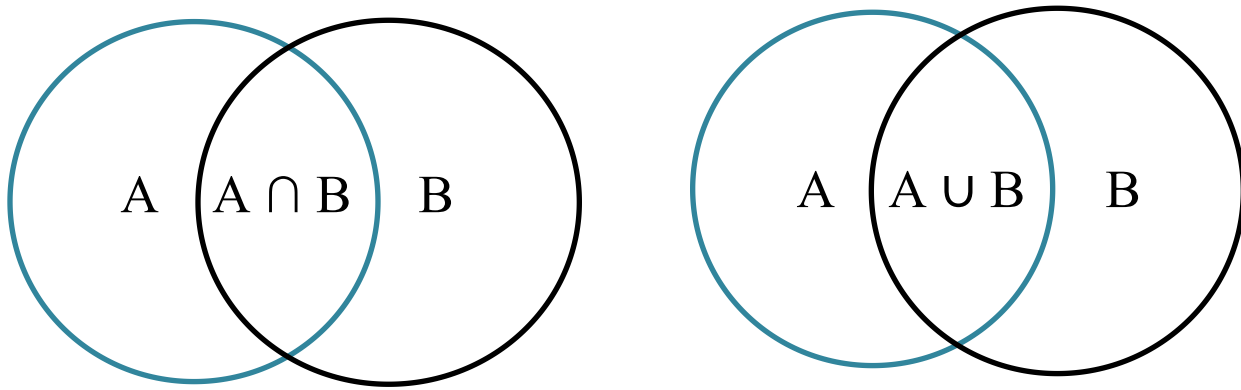
Here, score = bfscore(prediction,groundTruth) called scorer for better cure because it enumerates the BF(F1 boundary value) counter assimilated score between prediction's anticipated segmentation and groundTruth's true segmentation For binary segmentation prediction and groundTruth can be a pair of



logical arrays or can be said it's kind of category arrays for binary classification segmentation.

Jaccard Index:

When comparing a set of selected features for a sample to the relevant set of labels, the Jaccard Index is utilized. It is specified as the intersection's width split by the union's width between two sets.



$$J(A, B) = \frac{A \cap B}{A \cup B}$$

Fig 2.14: Jaccard similarity coefficient for set A and set B

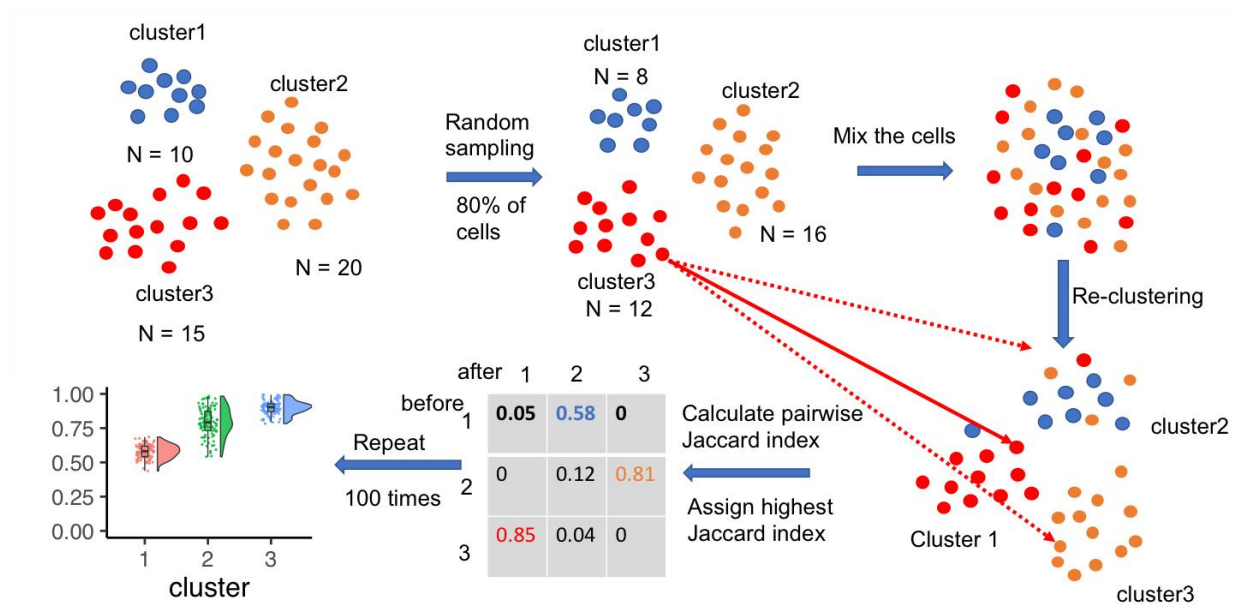


Fig 2.15: Uses of Jaccard similarity index/Jaccard index for 'single-cell cluster' stability using the Jaccard similarity index [43]

## 2.4 Relevant Research

When breast cancer is found, ultrasound imaging of the breast is typically used in conjunction with a physical examination and (X-ray) mammography [17]. Although traditional B mode ultrasound images can't justify transmogrification as efficiently as X-ray sonography which is actually a crucial sign of cancer, it is utilized to differentiate benign tumors from types of malignant tumors. Several clinical research have looked at how effectively masses may be defined by human viewers from a single image in terms of static image texture and geometric features. [18]–[20].

Horsch et al. [21] presents a technique for enhancing mass structures in a preprocessed image by thresholding it. On 400 cases/757 photos, a partially automatic and fully automatic version of the procedure is introduced, and a comparison with hand delineation is conducted. In those images 124 are complex in nature, 182 are benign & 94 malignant. Researchers analyse four image-based features (contour, echogenicity, margin, and posterior acoustic behavior), each specified in terms of the depth-to-width ratio, auto-correlation, "defined directional gradient," and gray-level comparison, to see if they can distinguish between cancerous and benign tumors. The advantages of unique features were studied using classification techniques in [22] and [23], and the best two features were found to be the complexity ratio (contours) and normalized radial gradient (margin). Drukker et al. [24] refined their work to include mass detection in later work targeted at further automating the procedure. They suggested first filtering the images with a directional gradient index filtering methods. [21] and [22] used the same database to test the approach. They discovered that 75% of lesions had been adequately recognized. For additional evaluation on a second database, see Drukker et al. [25]. The following are the major goals for developing an algorithm that can:

- I. Early detection is the key.
- II. Perform tumor segmentation fully automatically without any user intervention.
- III. Selects an automated threshold value for Watershed Method.

Because of we are measuring our detection accuracy with three precision matrices (Dice score, BF score, Jaccard Index). The harmonic mean (F1-measure) of the performance of the classifier values is used in conjunction with a distance error tolerance to determine whether a juncture on the expected boundary corresponds to the ground truth region in terms of BF score. We have detected more accuracy in the field of comparison set of predicted labels for a sample to the corresponding set of labels via Jaccard index values. We create an automated system to label a ground truth region in your image. The Dice score, which really is a measure of how similar objects are, is used to validate our algorithm.

After running a gray scale image to binary image in our algorithm, we have extracted some significant values where tumor detection shows more precision and accurate. From our two datasets [26-27], many categories BUS images have been undergone with the algorithm and we have found some precision matrices values which ensured us about the accuracy of our research.

# Chapter 3

## METHODOLOGY

### 3.1 Introduction

This research utilizes three parameters extracted from the power spectrum of ultrasound radio-frequency (RF) echo signals which are nothing but US images. Our two datasets provide many US images. From those images, we can differentiate between diverse types of tumors. And our system is time consuming. As we are measuring our detection accuracy with three precision matrices: Dice score, BF score, Jaccard Index.

To find those precision values we merged a few methods based on contrast, segmentate boundaries, shadows, and thresholding. Our algorithm is given below:

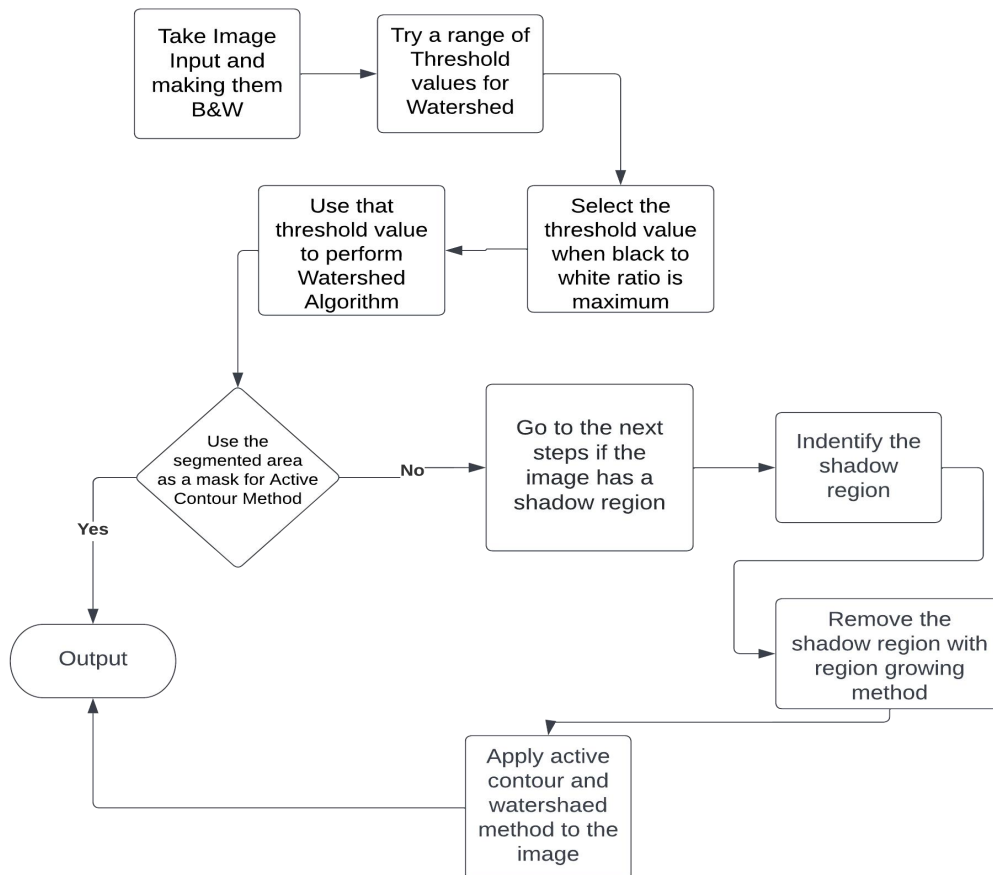


Fig 3.1: Our proposed algorithm flowchart

## 3.2 Data Collection

We have started our work with one data set [26] which we called Dataset-1. With this dataset-1 we did lot of experimental simulation via MATLAB and beside this our code was underdeveloped. After getting the code better than previous precision values, we used another dataset [27] which is Dataset-2.

Dataset-1[26] is comprised up of data acquired at baseline, including breast ultrasound scans from women aged 25 to 75. This information was gathered in 2018. There are 600 female patients in all. The collection includes 780 photos with an average image size of 500500 pixels. PNG files are used for the images. The photos are divided into three categories: normal, benign, and malignant. The number of photographs in each category is displayed in Table 3.1. The data samples were experimented and acknowledged are given in Fig. (3.2)

Table 3.1: The amount of photos in each of the three kinds of breast tumors

Case	No. of Images
Benign	487
Malignant	210
Normal	133
Total	780

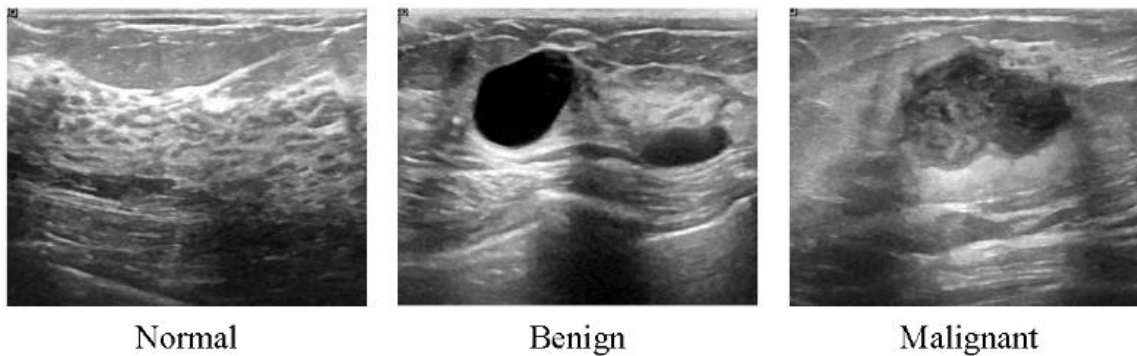


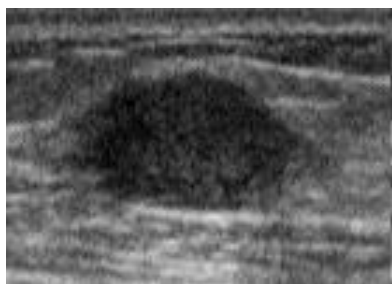
Fig 3.2: Samples of Ultrasound breast images data set

The total number of images collected at the start was 1100. The total number of images in the collection was reduced to 780 after pre-processing. The actual images contained irrelevant data that is not used in large scale segmentation. Furthermore, they may have an impact on the training process's output results. The LOGIQ E9 ultrasound technology and the LOGIQ E9 Agile ultrasound technology were implemented in the scanning procedure. These instruments are typically employed in high-end radiology, cardiac, and vascular imaging. They also have 1280\*1024 image resolution. On the ML6-15-D Matrix linear probe, the transducers varies from 1 to 5 MHz. Data set 2 contains 250 photos of breast cancer, 100 benign and 150 malignant. It is a database that is already widely utilized in numerous academic publications like in the field of Breast Ultrasonography.

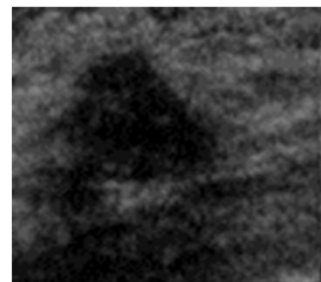
The data set must meet certain criteria in order to be efficient. The data set had identical images that needed to be replaced. The incorrect annotation was also examined and corrected by Baheya radiologists. DICOM pictures were transferred to PNG format using a DICOM converting tools[32]. Overall amount number of US photos was trimmed to 780 once the data set was refined. The photos are categorized into three categories: typical, benign, and malignant . To remove unnecessary and insignificant boundaries from the photographs, they were cropped to various sizes. For this work, we employed rapid photo crop [33]. The picture name is updated with the image annotation. All photos were evaluated and checked by professional radiologists at Baheya hospital [34].

### 3.3 Types of Images

Type 1:  
Images with no shadow Region



Type 2:  
Images with Shadow Region



### 3.4 How the algorithm works

To perform our algorithm perfectly we followed some steps:

Step 1: Taking the input of the images.

Step 2: To find the supreme threshold value respect to Watershed Method, At First, we try with different values. In our code, we choose values from 0.1 to 0.5 with 0.01 intervals.

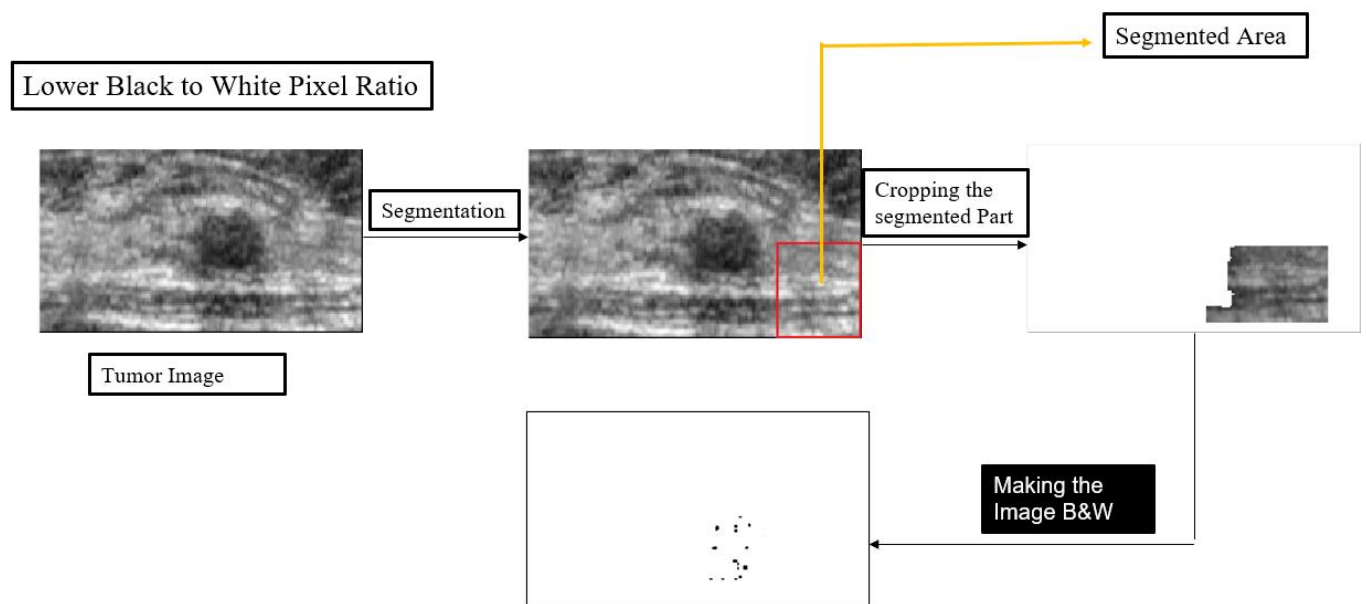


Fig 3.3: For finding the threshold value while segmented area has a large Black and White pixel ratio 1

Step 3: To find the right threshold value, we choose the value when the segmented area has a large black to white pixel ratio.

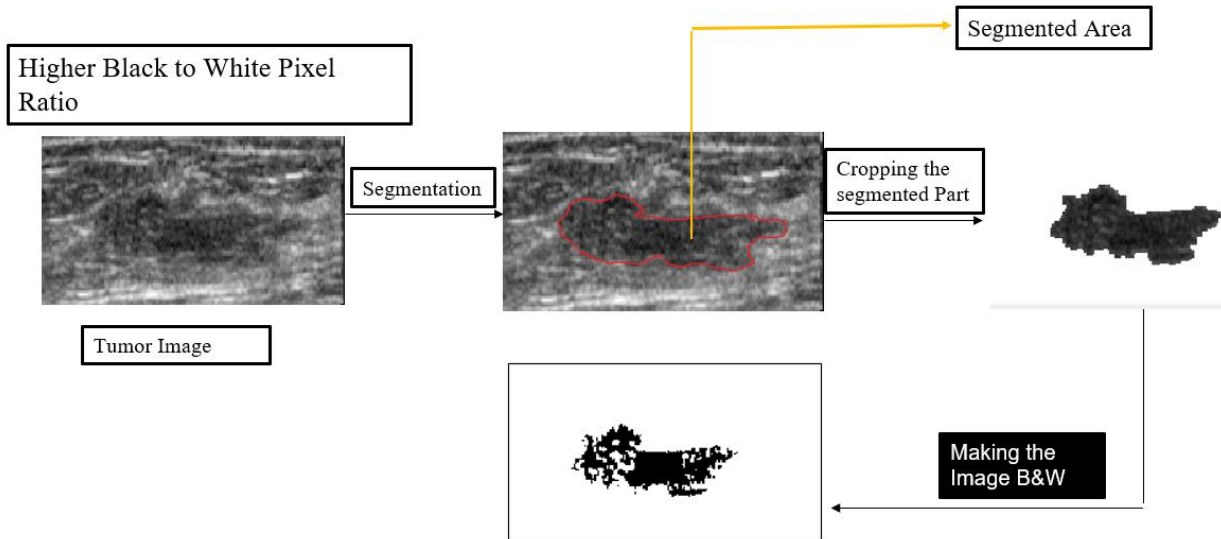


Fig 3.4: For finding the threshold value while segmented area has a large B&W pixel ratio 2

Step 4: When we have the right threshold value, from the previous step, we use it to find the Watershed Segmentation

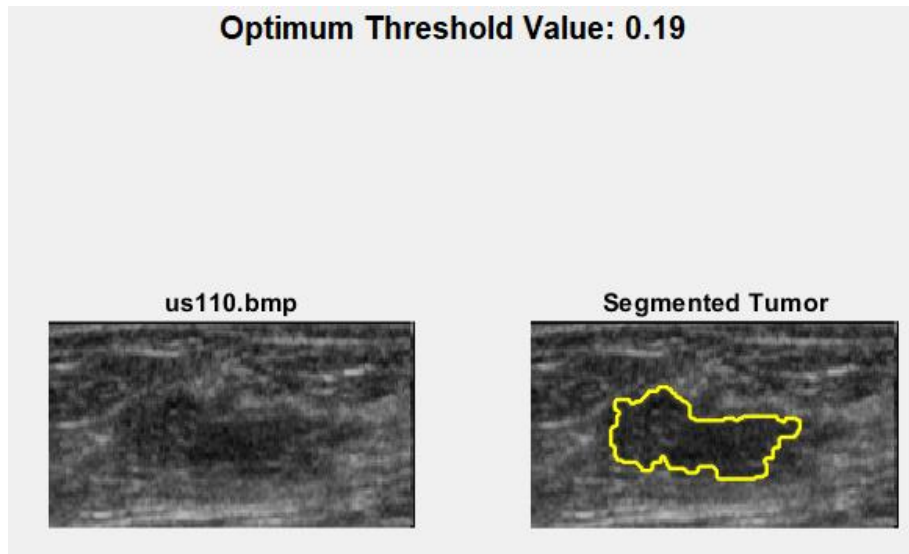


Fig 3.5: Segmented Image from dataset-1 (us110.bmp) in Matlab implementation



Step 5: Active Contour requires a ROI for segmentation. For precision, we apply the mask obtained from Watershed to the original tumor image.

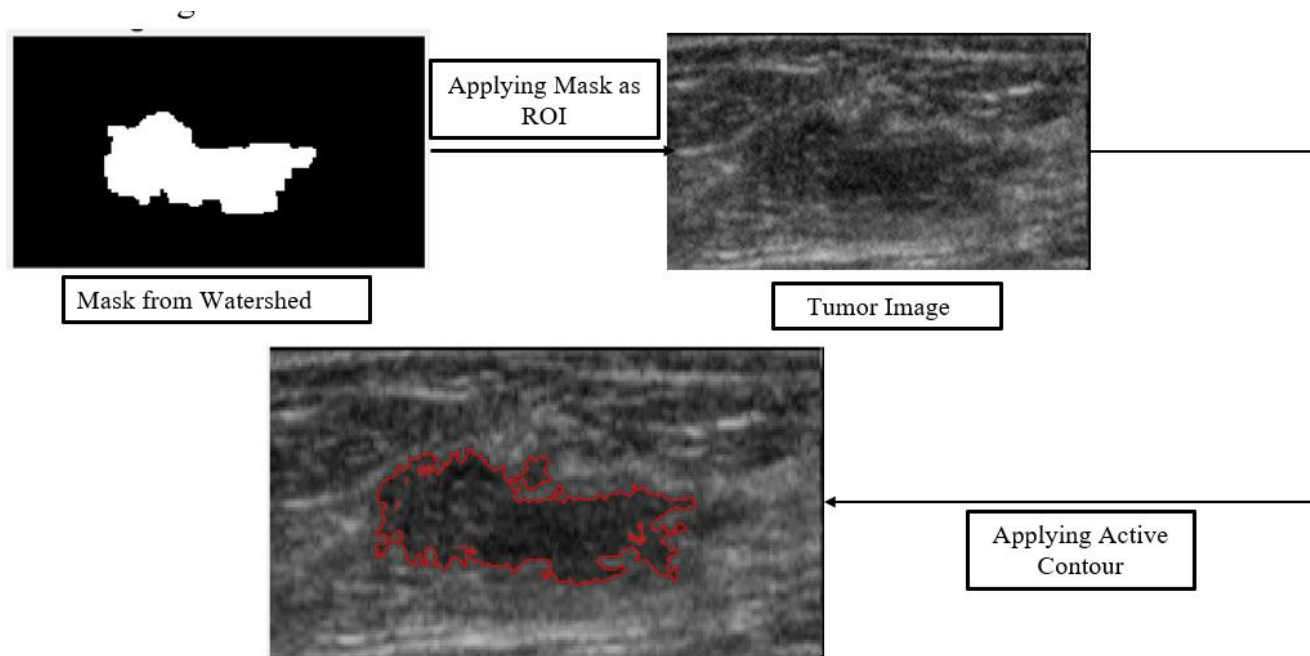
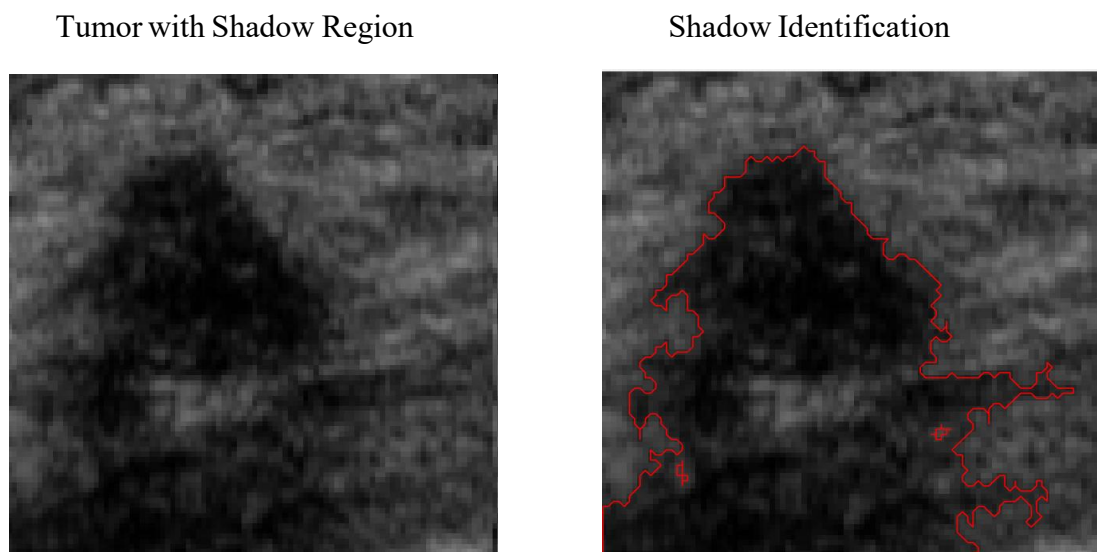


Fig 3.6: Active Contour requires a ROI for segmentation.

Step 6: Shadow Identification:



Step 7: Applying Region Growing Method for the border points as seeds.

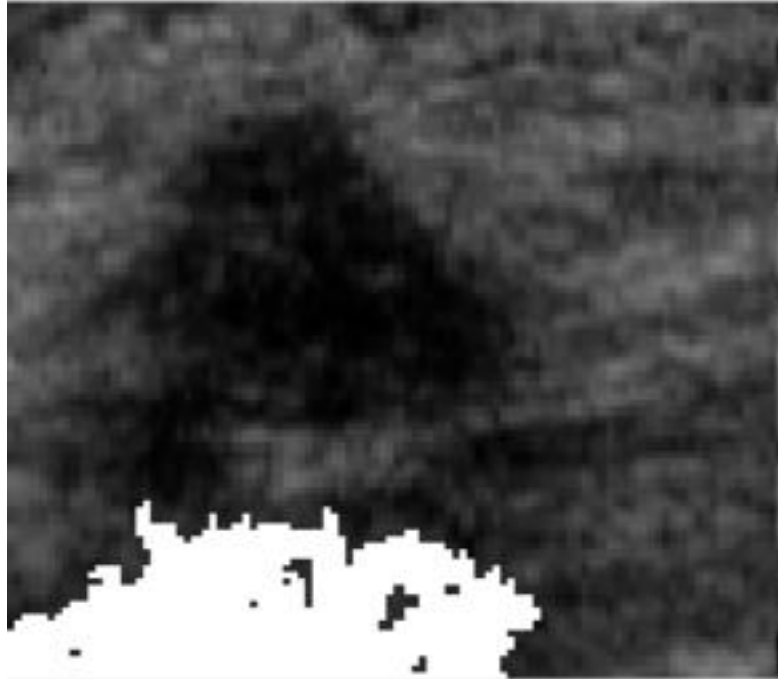


Fig 3.7: Shadow is removed using Matlab implementation

Step 8: Now, we apply Watershed- Active Contour Model to the shadow removed images.

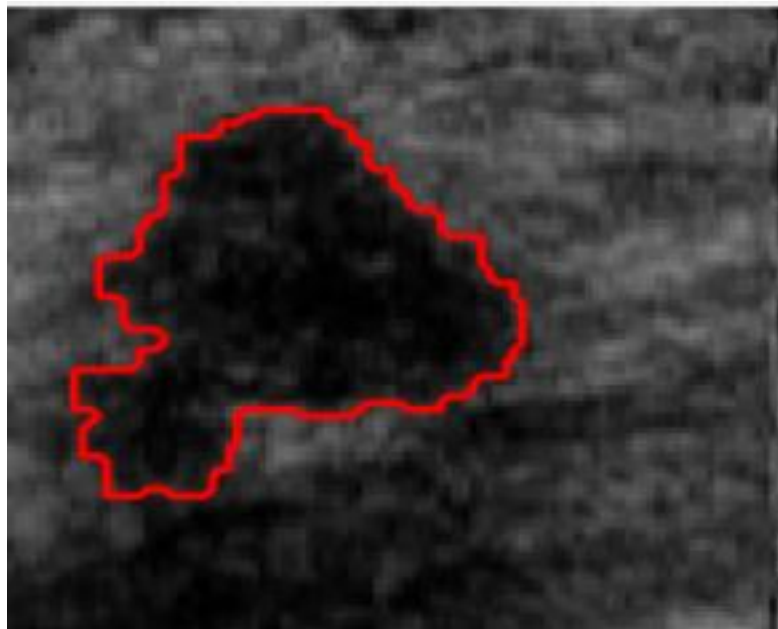


Fig 3.8: Watershed- Active Contour Model applied to the shadow removed images.

## Chapter 4

### RESULTS AND DISCUSSION

#### 4.1 Introduction

We have started our work with one data set [26] which we called Dataset-1. With this dataset-1 we did a lot of experimental simulation via MATLAB and beside this our code was underdeveloped. After getting the code better than previous precision values, we used another dataset [27] which is Dataset-2 .

#### 4.2 Results for Data samples

- For dataset 1 (without shadow)

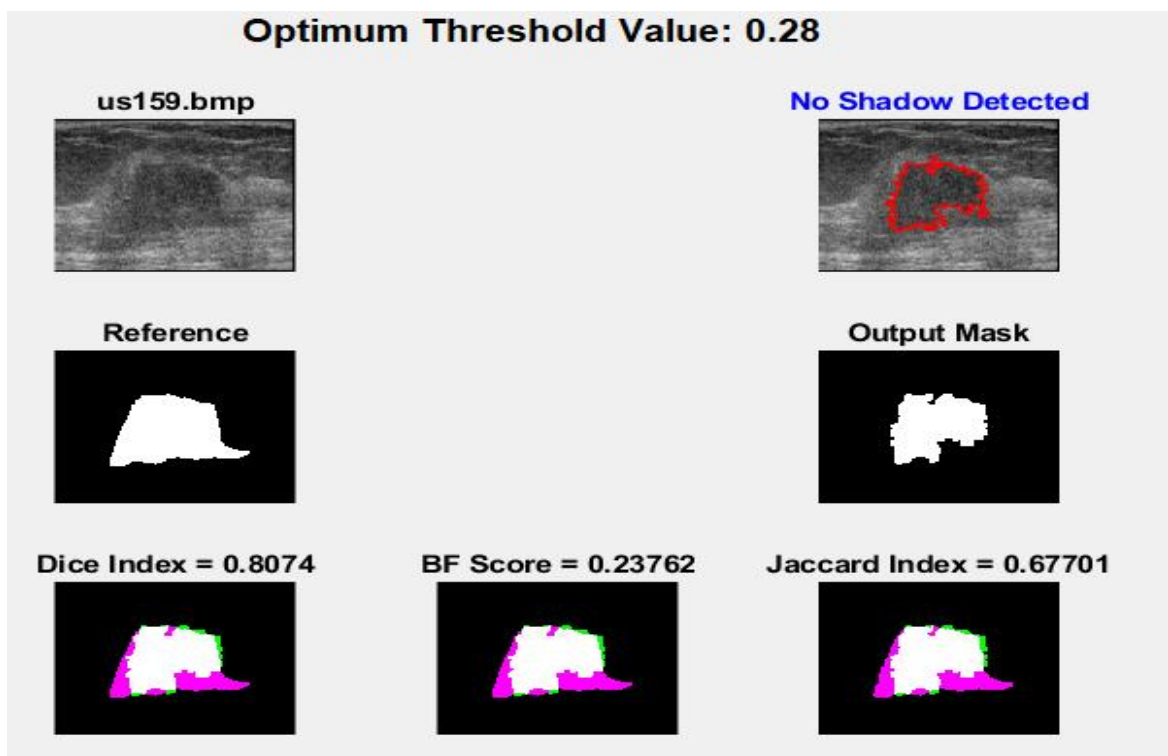


Fig 3.9: Image Without Shadow (us159.bmp)

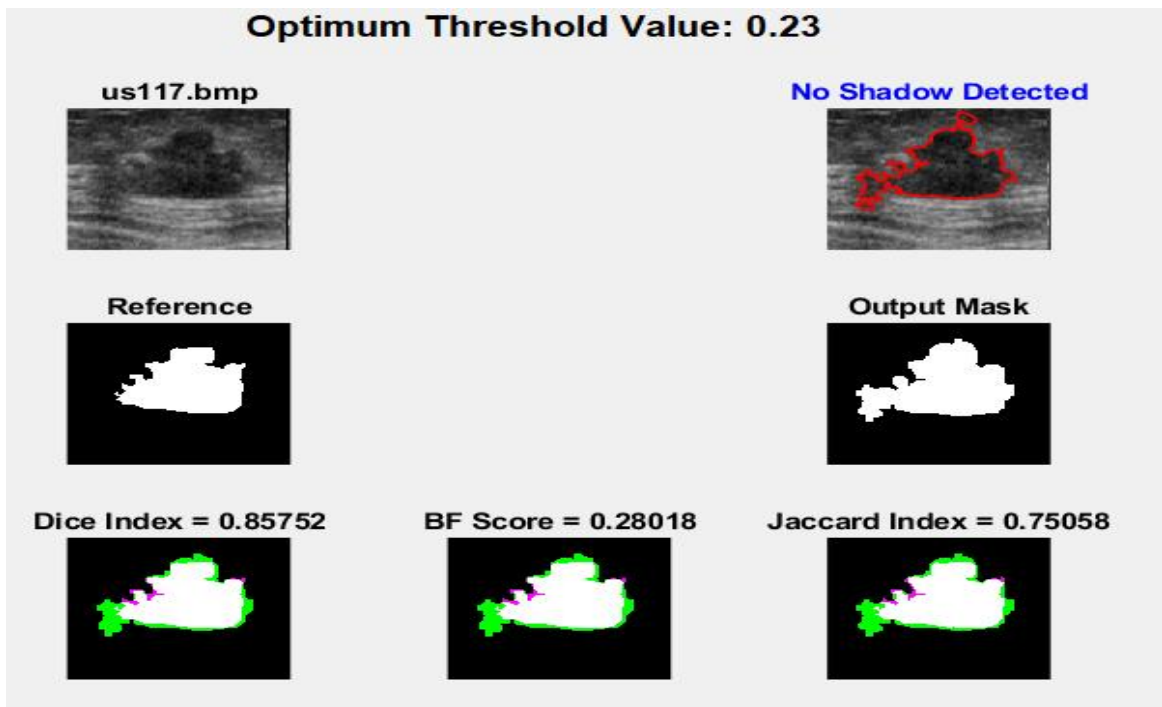


Fig 3.10: Image where no Shadow (us117.bmp)

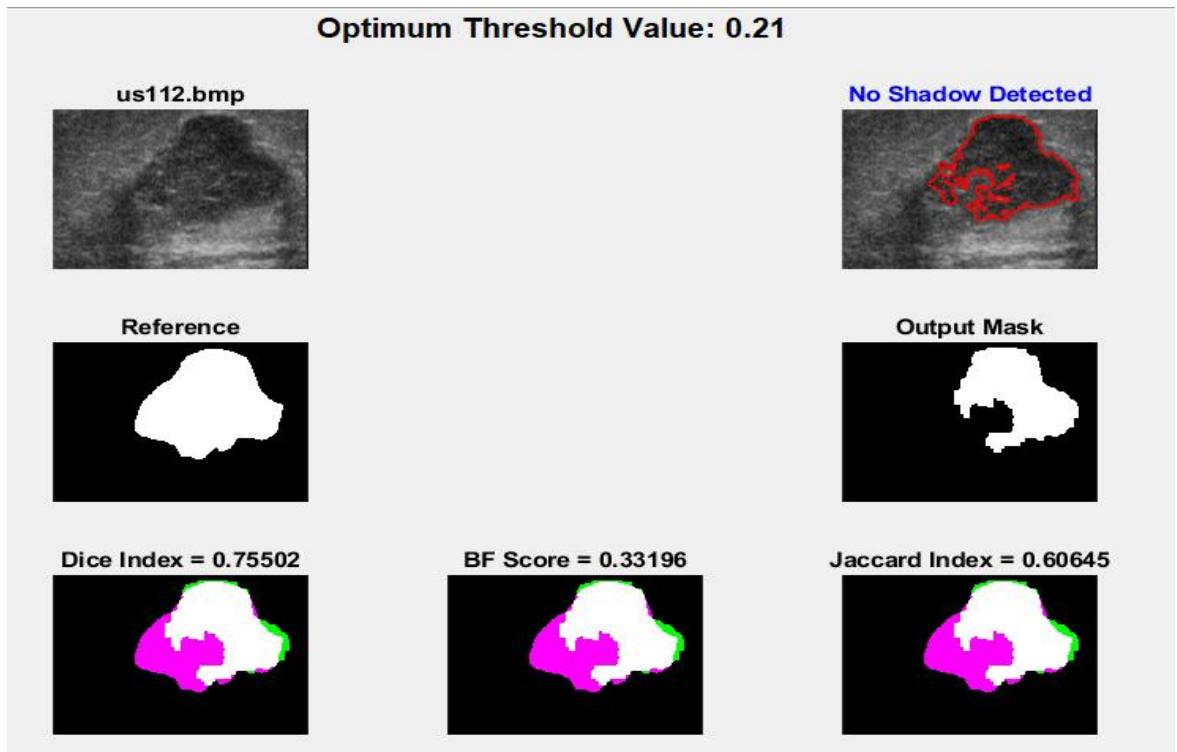


Fig 3.11: Image Without Shadow (us112.bmp)

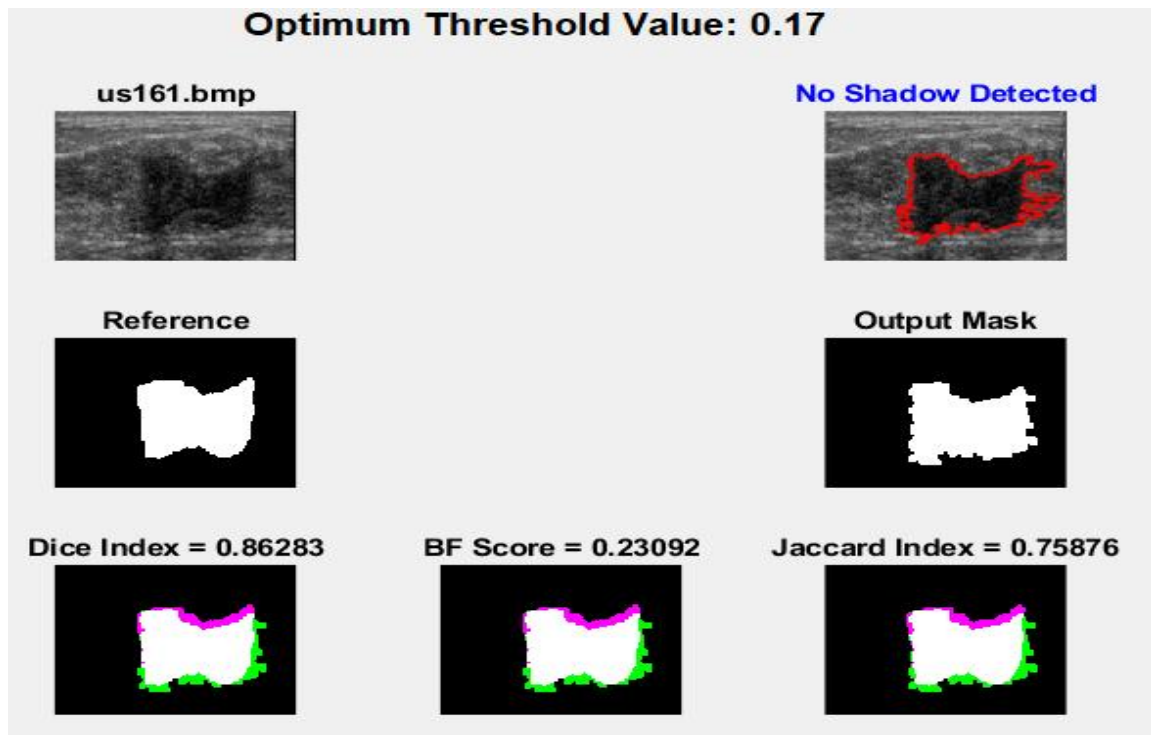


Fig 3.12: Image Without Shadow (us161.bmp)

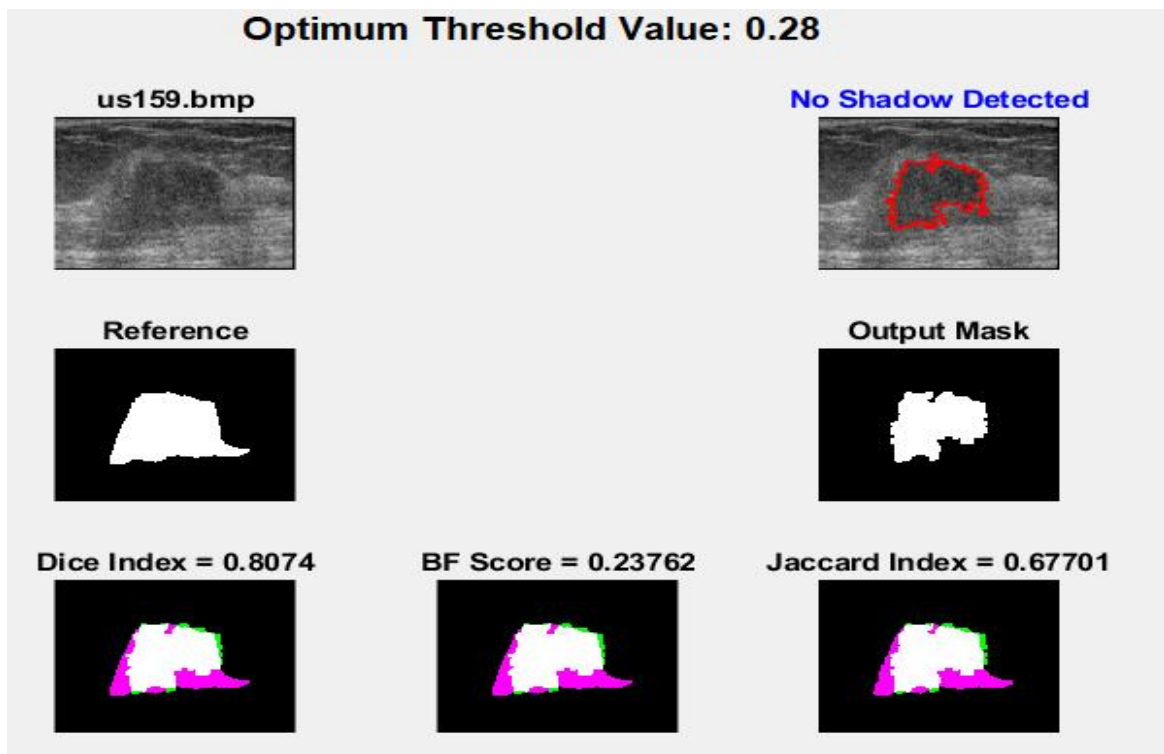


Fig 3.13: Image Without Shadow (us159.bmp)

➤ For dataset 1 [ Images with Shadow]

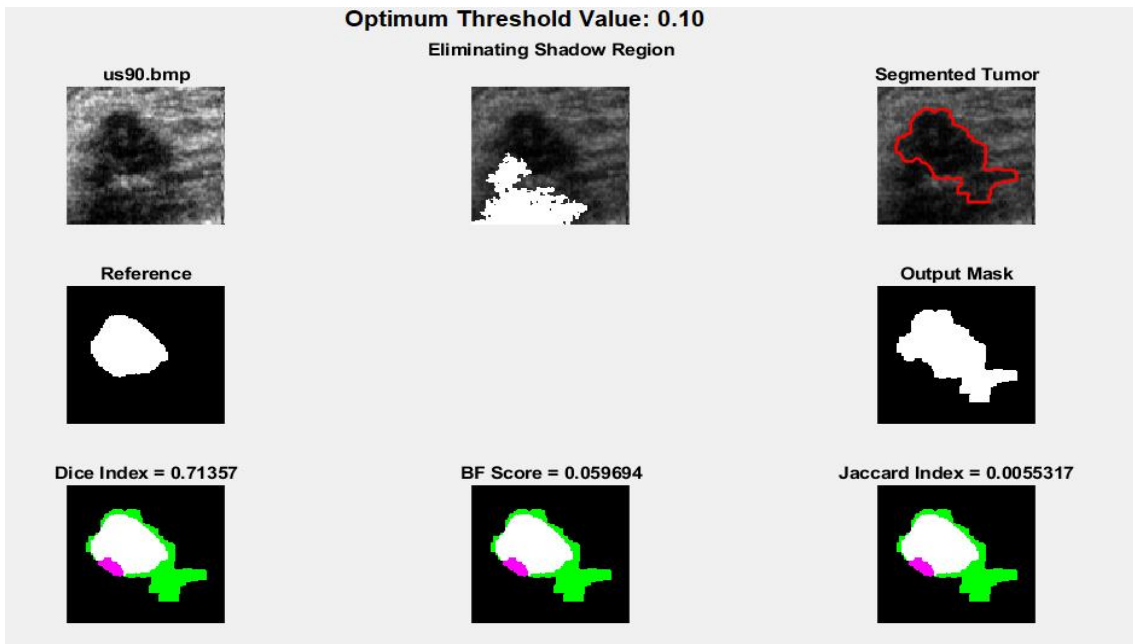


Fig 3.14: Image With Shadow Elimination (us90.bmp)

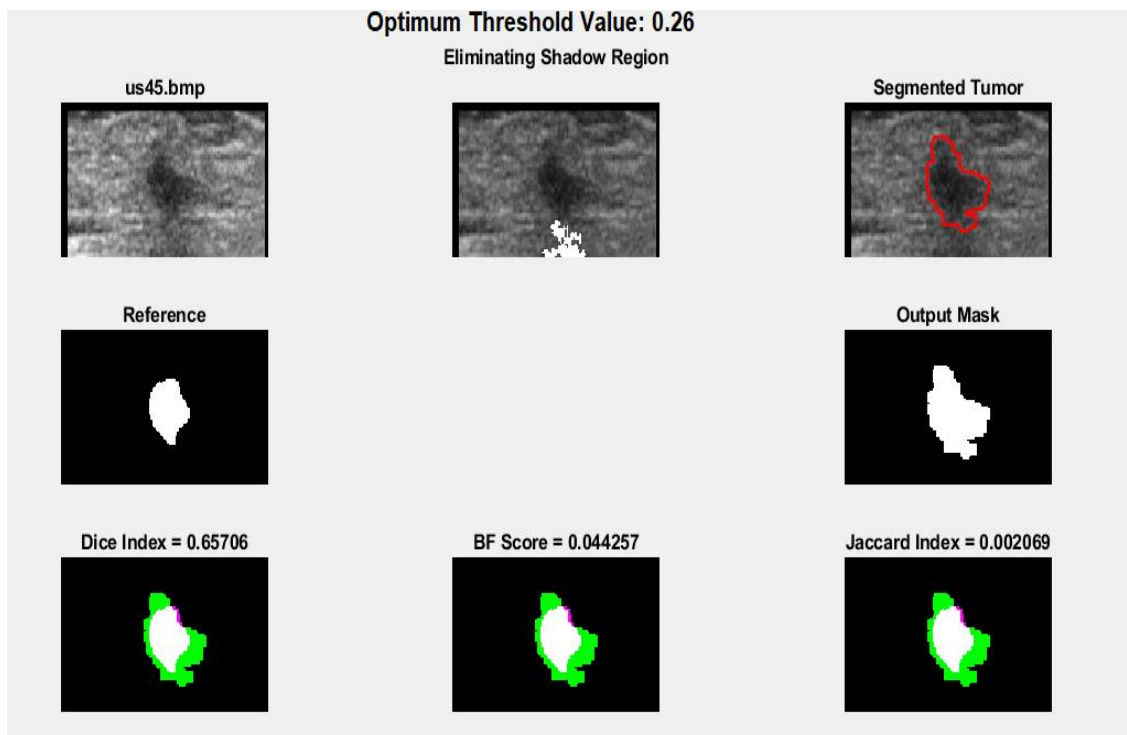


Fig 3.15: Image With Shadow Elimination (us45.bmp)

➤ For Dataset 2 [Image without shadow]

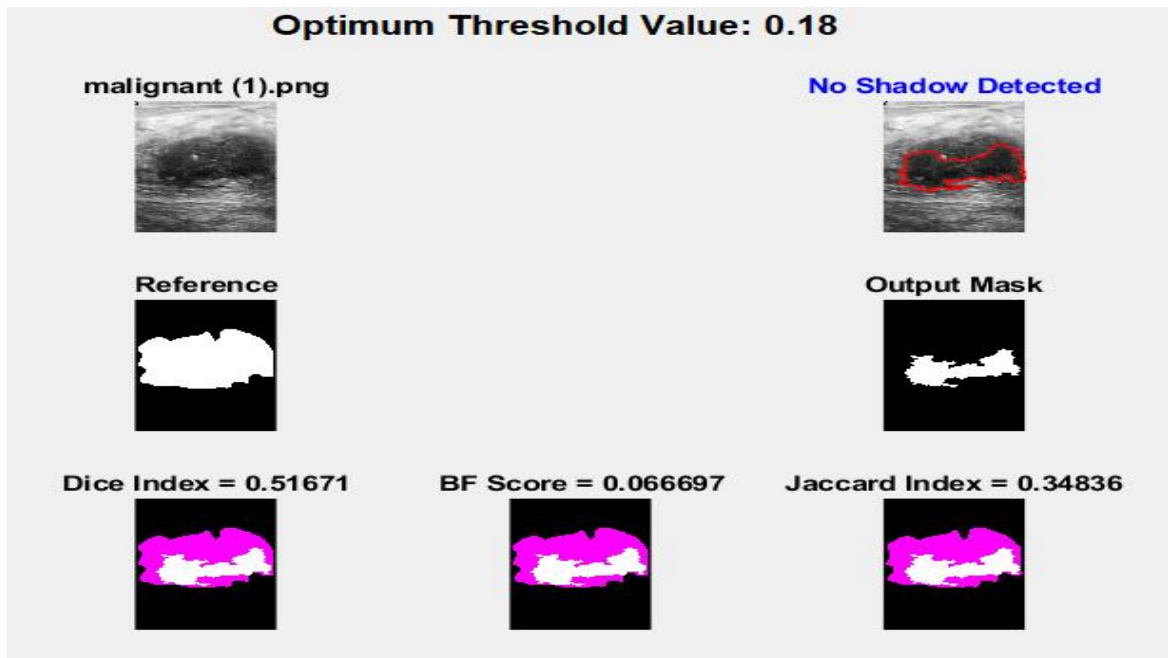


Fig 3.16: Image Without Shadow ( malignant(1).png )

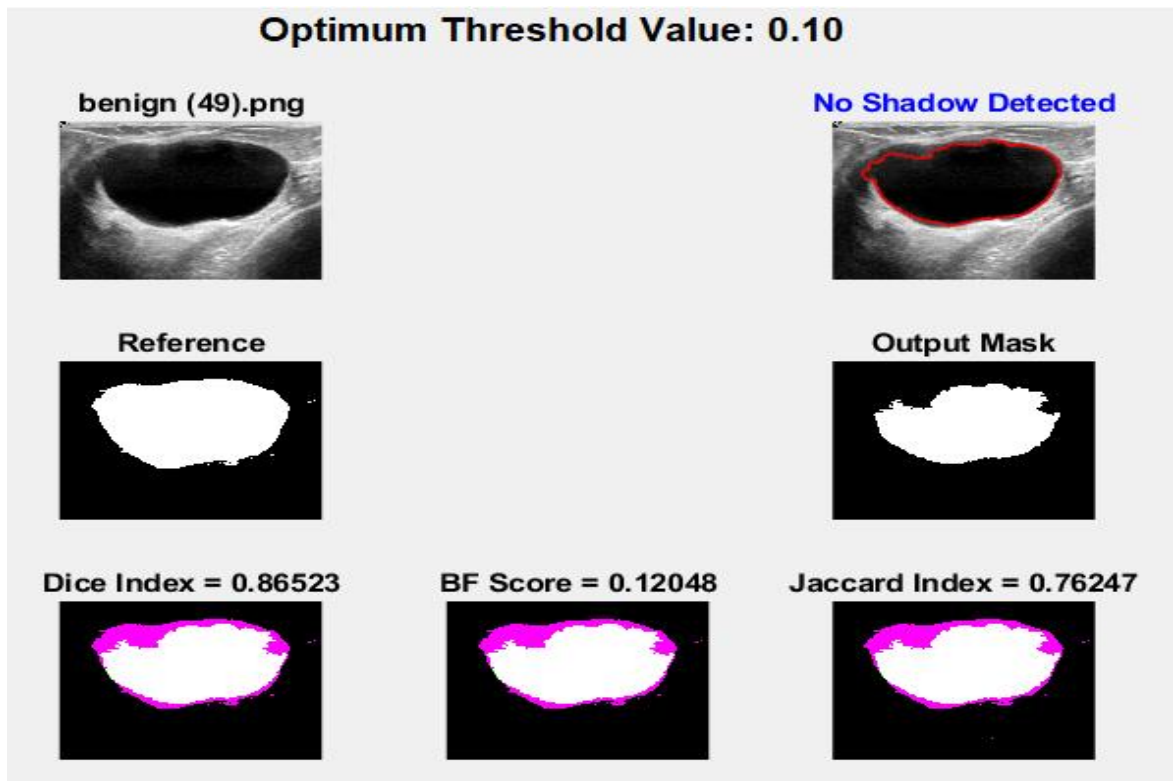


Fig 3.17: Image Without shadow ( benign(49).png )

➤ For Dataset 2 (Image with shadow):

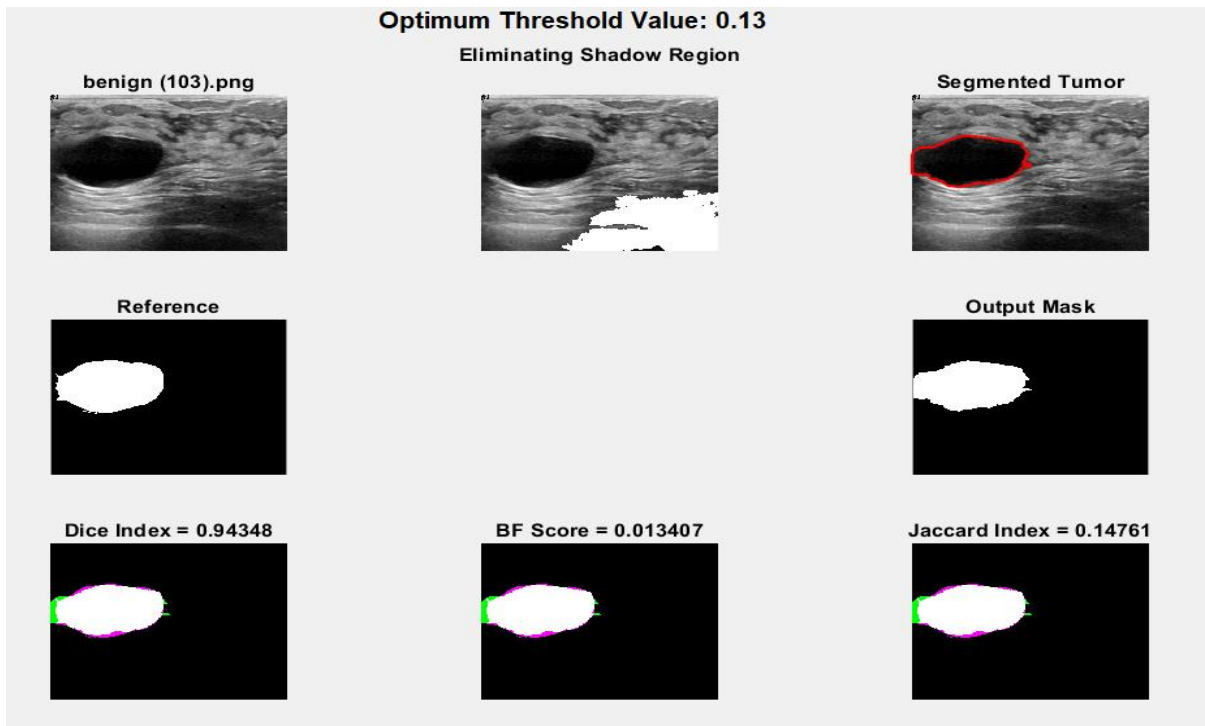


Fig 3.18: Image With Shadow Elimination ( benign(103).png )

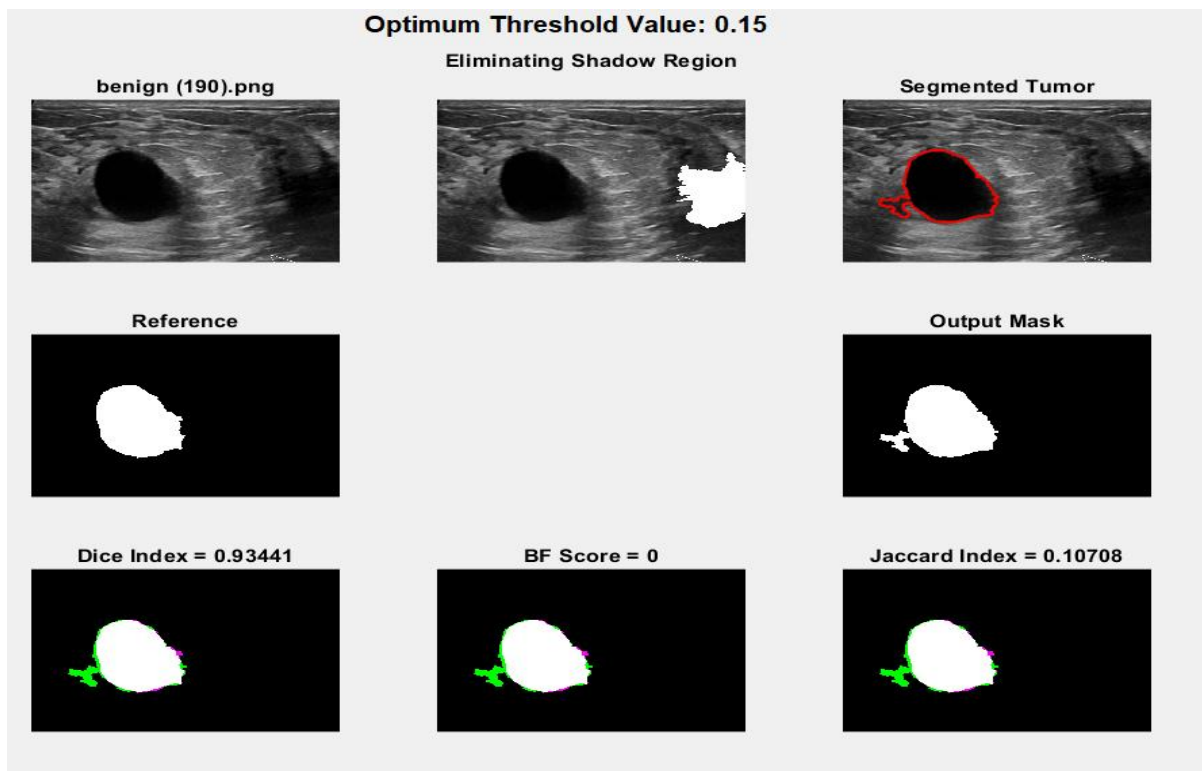


Fig 3.19: Image With Shadow\_Elimination ( benign(190).png )



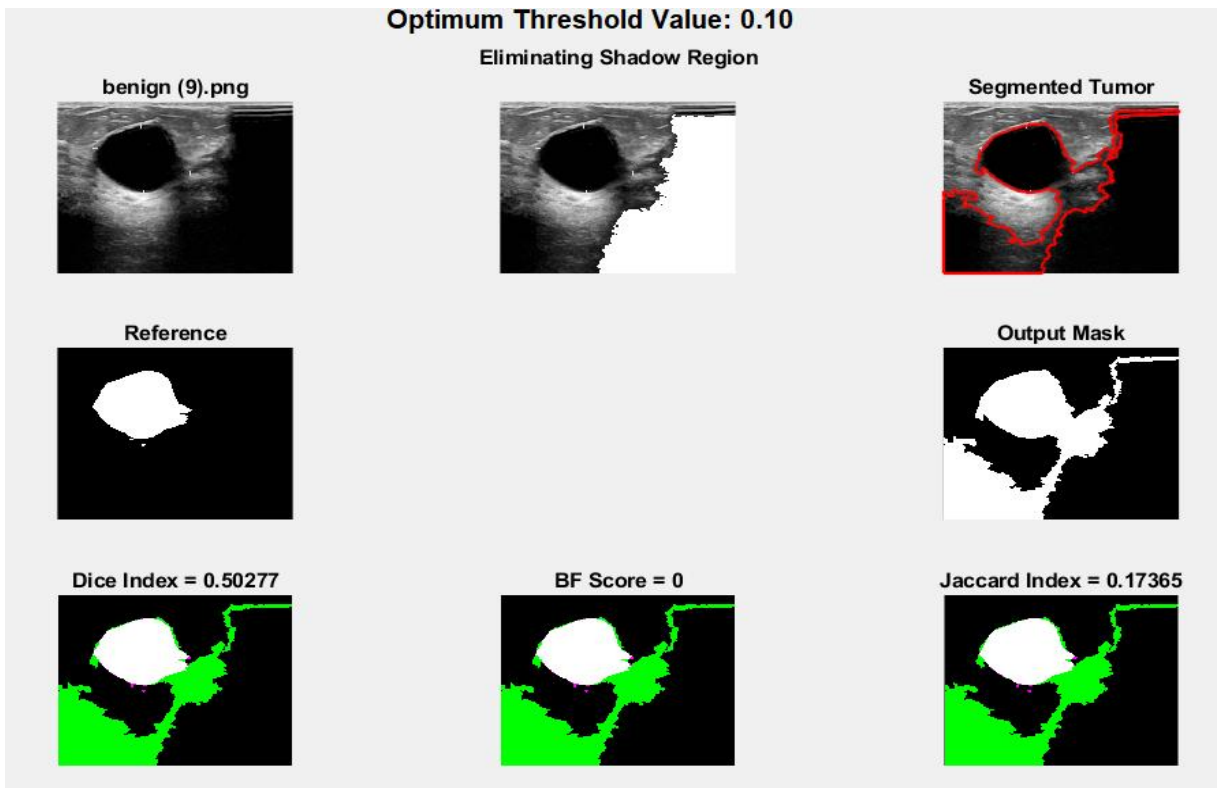


Fig 3.20: Image With Shadow Elimination ( benign(9).png )

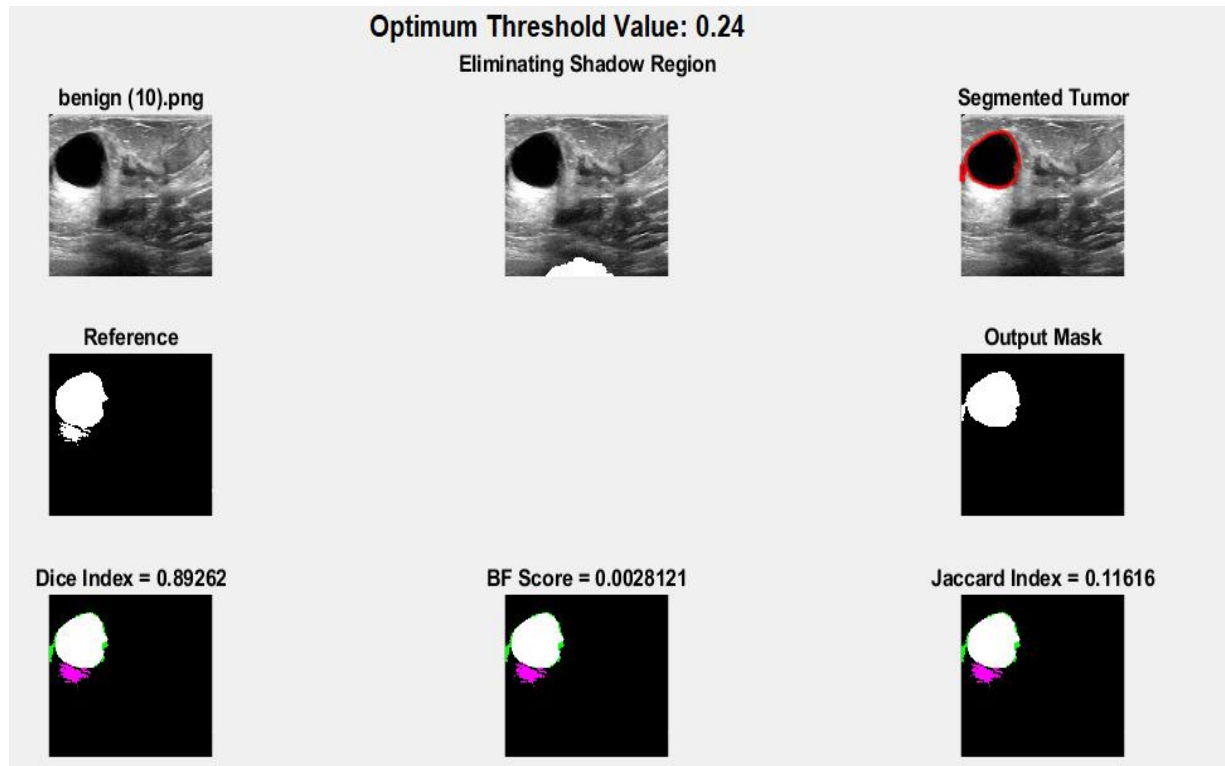


Fig 3.21: Image With Shadow Elimination ( benign(10).png )

### 4.3 Final Result

We have implemented our code using Matlab software and done various simulation using our Data sets. After simulating vast number of images our precision matrix ideology gave us some Following best values:

Table 4.1: Result of our Study

Dataset-1	Dataset-2
➤ Dice Score: 0.801403	➤ Dice Score: 0.795265
➤ BF Score: 0.18398	➤ BF Score: 0.0290565
➤ Jaccard Index: 0.475274	➤ Jaccard Index: 0.25793

### 4.4 Discussion

As we found the result respect to three parameters upon testing two database [26,27] ultrasound images, finally we could see the hope. The parameters of peak factors and power energy consistently achieved good levels of accuracy in diagnosing benign and malignant tumors for all three distinct sizes of ROI evaluated. To classify a ground truth region in the images, we develop an automated approach. The Dice score, which really is a measure of how similar objects are, is used to validate our algorithm. To ascertain if a point on the predicted edge matches the statistical data edge with regard to BF score, the fundamental average (F1-measure) of the efficiency of the perceptron values is employed in tandem with a proximity error tolerance. Furthermore, for respected samples, values of the parameter from the top region generated the greatest results in terms of classification accuracy.

## Chapter 5

### CONCLUSION

#### 5.1 Introduction

Integrated imaging modalities may be able to compensate for each other's shortcomings. First, according to the flexibility and real-time imaging capabilities of ultrasound, gas, sedimentation, and a variety of artifacts can be eliminated. Target lesions already detected by another imaging modalities can be reliably assessed using real-time picture fusion with ultrasound, which could lead to a variety of medical pertains. Moreover, ultrasonic embedding imaging allows to assist specimens to tumors which are only apparent with other regimens, eliminating the drawback of many other regimens, which is the inability to see the probe and lesion contact in real time. Third, an ultrasound fusion volume navigation technique can be employed to assess the breast tumors which need to be accompanied on. The generation of ultrasound images and its benefits in the medical profession were explored in this article. We need to improve the characteristics that we require for further processing because there are more applications in the field of ultrasound images for diagnosis and therapeutic purposes. There are various methods for accomplishing this. Segmentation, a broad topic of image processing, is one of them. So, we briefly reviewed segmentation methods in the last part. We explored various strategies after learning about segmentation and ultrasound images.

#### 5.2 Future scopes of Research

- Testing our algorithm against more datasets.
- Improving the accuracy scores [ F1, DICE scores] against other methods.
- Integrating deep learning algorithms for better performance.
- We assume shadow in the segmented region when the region touches boundary. Although this logic works for most cases, there are few cases where it doesn't. We plan on improving this aspect.

### 5.3 Conclusion

Our system proposes a promising aspect of tumor identification utilizing a quantitative approach based on factors taken from the power spectrum, with high percentages of classification accuracy. We understand that our algorithm has room for improvement. In future we would like to integrate more ideas to make the precision even better. We would like to thank our respected thesis supervisor Professor Dr. Taslim Reza Sir for his impeccable assistance and encouragement. We hope that our algorithm can be used to finesse the process of segmentation.

## References

- [1] Center for Disease Control and Prevention. Cancer among women. Cancer Prevention and Control website. [www.cdc.gov/cancer/dcpc/data/women.htm](http://www.cdc.gov/cancer/dcpc/data/women.htm). Published January 2, 2013. Accessed October 7, 2013
- [2] International Agency for Research on Cancer. Breast cancer incidence, mortality and prevalence Worldwide in 2008. GLOBOCAN website. [globocan.iarc.fr/Pages/fact\\_sheets\\_cancer.asp](http://globocan.iarc.fr/Pages/fact_sheets_cancer.asp). Published July 10, 2013. Accessed October 7, 2013
- [3] R. L. Siegel, K. D. Miller and A. Jemal, "Cancer statistics, 2016," *CA Cancer J Clin*, vol. 66, no. 1, pp. 7-30, 2016.
- [4] C.M. Sehgal, S.P. Weinstein, P.H. Arger, E.F. Conant, A review of breast ultrasound, *J. Mammary Gland Biol. Neoplasia* 11 (2006) 113–123.
- [5] J.G. Bosch, S.C. Mitchell, B.P. Lelieveldt, F. Nijland, O. Kamp, M. Sonka, J.H. Reiber, Automatic segmentation of echocardiographic sequences by active appearance motion models, *IEEE Trans. Med. Imaging* 21 (2002) 1374–1383.
- [6] Kisslo J, Firek B, Ota T, Kang DH, Fleishman CE, Stetten G, Li J, Ohazama CJ, Adams D, Landolfo C, Ryan T, von Ramm O. Realtime volumetric echocardiography: The technology and the possibilities. *Echocardiography* 2000;17:773–779.
- [7] T. Chan and L. Vese, "Active contours without edges," in *IEEE transactions on imageprocessing* 10(2), 2001, pp. 266-277.
- [8] Active Contours Without Edges | Sanjay Chaudhary - Academia.edu
- [9] Md. Anisur Rahman Farazy, "Incidence of Breast Cancer in Bangladesh," *Health Care*, vol. 3, issue 3, pp. 53-54, October, 2015.
- [10] American Cancer Society, in *Cancer Facts and Figures*, 2019.
- [11] Siegel RL, Miller KD & Jemal A, "Cancer Statistics, 2019," *CA Cancer J Clin*, vol. 69, issue 1, pp. 7 – 34, 2019.
- [12] Ultrasound Imaging FDA. (<https://www.fda.gov/radiation-emitting-products/medical-imaging/ultrasound-imaging>) (accessed May 1,2022)
- [13] Propagation of Sound Waves (<https://www.pasco.com/products/guides/sound-waves>) (accessed April 27,2022)

- [14] Instrumentation\_Electronics/transducer/2011/07.(<http://www.instrumentationtoday.com/piezo-electric-transducer/2011/07>) (accessed May 1,2022)
- [15] Carstensen, E. L. (1976). Interaction of Ultrasound with Tissues. *Ultrasound in Medicine*, 517–517.
- [16] Interaction\_of\_Ultrasound\_Waves\_with\_Tissue.(<https://eechocardiography.com/page/page.php?UID=1427121051>) (accessed May 5,2022)
- [17] B. D. Fornage, “Ultrasound of the breast,” *Ultrasound Quart.*, vol. 11, no. 1, pp. 1–39, 1993.
- [18] A. Stavos, D. Thickman, C. Rapp, M. Dennis, S. Parker, and S. G.A., “Solid breast modules: Use of sonography to distinguish between benign and malignant lesions,” *Radiology*, vol. 196, pp.123–134,1995.
- [19] V. Jackson, “Management of solid breast modules: What is the role of sonography? *Radiology*, vol. 196, pp. 14–15, 1995.
- [20] P. Arger,C. Sehgal, E. Conant, J. Zuckerman, S. Rowling, and J. Patton, “Interreader variability and predictive value of is descriptions of solid masses: Pilot study,” *Acad. Radiol.*, vol. 8, pp. 335–342, 2001
- [21] K. Horsch, M. L. Giger, L. A. Venta, and C. J. Vyborny, “Automatic segmentation of breast lesions on ultrasound,” *Med. Phys.*, vol. 28, no.8, pp. 1652–1659, Aug. 2001.
- [22] ———, “Computerized diagnosis of breast lesions on ultrasound,” *Med. Phys.*, vol. 29, no. 2, pp. 157–164, Feb. 2002.
- [23] K. Horsch, M. L. Giger, C. J. Vyborny, and L. A. Venta, “Performance of computer-aided diagnosis in the interpretation of lesions on breast sonography,” *Acad. Radiol.*, vol. 11, no. 3, pp.272–280, Mar. 2004.
- [24] K. Drukker, M. L. Giger, K. Horsch, C. J. Kupinski, M. A. Vyborny, and E. B. Mendelson, “Computerized lesion detection on breast ultrasound,” *Med. Phys.*, vol. 29, no. 7, pp. 1438–1446, Jul. 2002.
- [25] K. Drukker, M. L. Giger, C. J. Vyborny, and E. B. Mendelson, “Computerized detection and classification of cancer on breast ultrasound,” *Acad. Radiol.*, vol. 11, no. 5, pp. 526–535, May 2004.
- [26] Rodrigues, Paulo Sergio (2017), “Breast Ultrasound Image”, Mendeley Data, V1, DOI: 10.17632/wmy84gzngw.1
- [27] Al-Dhabyani W, Gomaa M, Khaled H, Fahmy A. Dataset of breast ultrasound images. *Data in Brief*. 2020 Feb;28:104863. DOI: 10.1016/j.dib.2019.104863.
- [28] Image Processing with Python.
- [29] Articles:“Watershed\_Algorithm\_and\_its\_application”.

(<https://www.aegissofttech.com/articles/watershed-algorithm-and-limitations.html>)

(accessed May 5,2022)

[30] Olivier Rousseau and Yves Bourgault, "Heart segmentation with an iterative Chan-Vese algorithm," University of Ottawa, Ontario , 2009.

[31] Fan, M., & Lee, T. C. M. (2015). Variants of seeded region growing. *IET Image Processing*, 9(6), 478–485. doi:10.1049/iet-ipr.2014.0490

[32] Medixant, RadiAnt DICOM Viewer, (2018). ([www.radiantviewer.com](http://www.radiantviewer.com)) (accessed May 5,2022)

[33] Śmieszny, Fast Photo Crop, 2013. (<https://apps.microsoft.com/store/detail/fast-photo-crop/9WZDNCRDNPV?hl=ar-eg&gl=EG>) (accessed May 3,2022)

[34] Al-Dhabyani, W., Gomaa, M., Khaled, H., & Fahmy, A. (2019). Dataset of Breast Ultrasound Images. *Data in Brief*, 104863. doi:10.1016/j.dib.2019.10486

[35] Diagnostics of pregnancy Pregnant woman getting ultrasound from doctor Ultrasound Stock Photo.(<https://media.istockphoto.com/photos/diagnostics-of-pregnancy-picture-id123824128>) (accessed May 5,2022)

[36] ‘Roshni's Physics E-Portfolio’. (<https://sites.google.com/site/roshnisphysicseportfolio/sound-waves>) (accessed May 5,2022)

[37] Fastest Anesthesia & Intensive Care & Emergency Medicine Insight Engine. (<https://aneskey.com/ultrasound-basics-2/#ch02ref1>) (accessed May 2,2022)

[38] Ultrasound Theory Module\_FAMUS.(<http://famus.org.uk/modules/ultrasound-theory-module>) (accessed April 29,2022)

[39] “Ultrasonic Materials Ideal for today’s highest- performance transducers\_ datasheet ultrasonic metaterials-10997 by Entegris’ POCO Materials are ideal for several high- technology industries.”

[40] Yao, Guilin. (2017). A Survey on Pre-Processing in Image Matting. *Journal of Computer Science and Technology*. 32. 122-138. 10.1007/s11390-017-1709-z.

[41] #007 OpenCV projects – Image segmentation with Watershed algorithm.

- [42] Al-Dhabyani, W., Gomaa, M., Khaled, H., & Fahmy, A. (2019). Dataset of Breast Ultrasound Images. *Data in Brief*, 104863.
- [43] “Ming Tang, Yasin Kaymaz, Brandon L Logeman, Stephen Eichhorn, Zhengzheng S Liang, Catherine Dulac, Timothy B Sackton, Evaluating single-cell cluster stability using the Jaccard similarity index, *Bioinformatics*, Volume 37, Issue 15, 1 August 2021, Pages 2212–2214”



## APPENDIX A

Code:

```
%%%%%%%%% Specifying the folder where the tumor images are. %%%%%%%%%%
imageLocation = 'F:\Study\matlab\Dataset_BUSI_with_GT\benign';

%%%%%%%%% Specifying the folder where the mask images are. %%%%%%%%%%
maskLocation = 'F:\Study\matlab\Dataset_BUSI_with_GT\benign\mask';

% Check to make sure that folder actually exists. Warn user if it doesn't.
if ~isfolder(imageLocation)
    Message = sprintf('Invalid Folder Location!', imageLocation);
    uiwait(warndlg(Message));
    imageLocation = uigetdir(); % Ask for a new one.
    if imageLocation == 0
        % User clicked Cancel
        return;
    end
end

%%%%%%%%% Show error message if folder location is invalid %%%%%%%%%%
if ~isfolder(maskLocation)
    Message = sprintf('Error: The following folder does not exist:\n%s\nPlease specify a new folder.',
maskLocation);
    uiwait(warndlg(Message));
    maskLocation = uigetdir();
    if maskLocation == 0

        return;
    end
end

%%%%%%%%% Keeping the variables constant at the start of each loop %%%%
minimum=0;
iteration=50;
thres=0;

%%%%%%%%% Get a list of all files in the folder with the desired file name pattern. %%%%%%%%%%
```

```

imageType = fullfile(imageLocation, '*.png'); %%% Specifying the image type
images = dir(imageType);

maskType = fullfile(maskLocation, '*.png'); % Change to whatever pattern you need.
masks = dir(maskType);

%%%%%% Starting a loop for the k number of image input %%%
for k = 1 : length(images)
    imageName = images(k).name;
    imageFullName = fullfile(images(k).folder, imageName);
    fprintf(1, 'Now reading %s\n', imageFullName);

    img = imread(imageFullName);
    [rows, columns, C_channels] = size(img);
    img = imread(imageFullName);

    %%% Finding out if the image is gray or not. If rgb, then convert to gray %%%
    [rows, columns, C_channels] = size(img);
    if C_channels > 1

        gray = rgb2gray(img);
    end
    if C_channels == 1
        gray = img;
    end
end
[rows, columns, numberOfColorBands] = size(img);
s=1;
w=1;
%%%%%% Applying Watershed Method for Threshold Values ranging from 0.1 to 0.5 with 0.01
interval %%%
for q=0.1:0.01:0.5
    bnw = im2bw(img,q);
    inv_bnw= ~bnw;
    C= -bwdist(inv_bnw);
    C(inv_bnw)= -Inf;
    M= watershed(C);
    Wi= label2rgb(M,'jet','c');%to visualize the label

    img_label=bwlabel(M);
stats=regionprops(img_label,'Solidity','Area');

```

```

dens=[stats.Solidity];
img_area=[stats.Area];
high_dense_area=dens>0.45; %We are taking 0.45 as the solidity value
maximum_area=max(img_area(high_dense_area)); %returns maximum area
tumor_label=find(img_area==maximum_area);
seg_tumor=ismember(img_label,tumor_label
se=strel('square',5);
seg_tumor=imdilate(seg_tumor,se);
[B,M]=bwboundaries(seg_tumor,'noholes'); % Creating a boundary around the segmented tumor
%%%%%%%%% Determining Boundary of Tumor %%%%%%%%%%
for i=1:length(B)
    [rows, columns, numberOfColorChannels] = size(img);
    seg_mask = poly2mask(B{i}(:,2),B{i}(:,1), rows, columns);
end
Boundary = B{1};
x = Boundary(:, 2);
y = Boundary(:, 1);
yellowMask = poly2mask(x, y, rows, columns);
pixelsInyellowMask = bnw(yellowMask);

%%%%%%%%% numBlack and numWhite are the number of black and white pixels respectively within the
segmented area %%%%%%%%%%
numBlack = sum(pixelsInyellowMask == 0);
numWhite = sum(pixelsInyellowMask == 1);

value(s)=q;

%%%%%%%%% Setting the Condition to Select The Optimum Threshold Value %%%%%%%%%%
    if(numBlack>numWhite)
        possibleOutput(w)=q;
        w=w+1;
    end

s=s+1;
end

%%%%%%%%% Finding the threshold value with the highest numBlack to numWhite ratio %%%%%%%%%%5
minimum=min(possibleOutput);
loc=find(value==minimum);
thresh(k)=value(loc);
end

```

```

%% Applying the same code again with the Optimum Threshold Value found in previous
steps %%%55
t=1;
m=1;

for k = 1 : length(images)
    imageName = images(k).name;
    imageFullName = fullfile(images(k).folder, imageName);
    fprintf(1, 'Now reading %s\n', imageFullName);

    for k = 1 : length(masks)
        basemaskFileName = masks(k).name;
        fullmaskFileName = fullfile(masks(k).folder, basemaskFileName);
        fprintf(1, 'Now reading %s\n', fullmaskFileName);
        maskimageArray = imread(fullmaskFileName);
        maskimage = rgb2gray(maskimageArray);
        maskimage=maskimage>250;
        img = imread(imageFullName);
        if C_channels > 1

            gray = rgb2gray(img);
        end
        if numberOfColorChannels == 1
            gray = img;
        end
        bnw=im2bw(img,thresh(k));
        inv_bnw= ~bnw;
        C= -bwdist(inv_bnw);
        C(inv_bnw)= -Inf;
        M= watershed(C);
        Wi= label2rgb(M,'jet','c');
        img_label=bwlabel(M);
        stats=regionprops(img_label,'Solidity','Area');
        dens=[stats.Solidity];
        img_area=[stats.Area];
        high_dense_area=dens>0.5;
        maximum_area=max(img_area(high_dense_area));
        tumor_label=find(img_area==maximum_area);
        seg_tumor=ismember(img_label,tumor_label);
        se=strel('square',5);
        seg_tumor=imdilate(seg_tumor,se);
    end
end

```

```

[B,M]=bwboundaries(seg_tumor,'noholes');
for i=1:length(B)
    [rows, columns, numberOfColorChannels] = size(img);
    seg_mask = poly2mask(B{i}(:,2),B{i}(:,1), rows, columns);
end
finalmask=seg_mask;
white = (seg_mask == 1);
numpixel=numel(seg_mask);
t=1;
i=3;
shadow=0;
p=1;
xup=[];
yup=[];
xdown=[];
ydown=[];
xleft=[];
yleft=[];
yright=[];
yright=[];
finalwhite=[];
xaxis=[];
yaxis=[];
%%%%%%%% Determining whether the tumor image has shadow or not %%%%%%%%%%
sidelen=[];
    for j=i:rows
        if seg_mask(j,columns)~=0

            shadow=1;
            xright(t)=columns;
            yright(t)=j;
            t=t+1;
        end

%%%%%%%% Determining shadow by finding out which side the segmented area touches (up, down, left or
right) %%%%%%%%%%5

    end
    if(shadow==1)
        sidelen(1) = t-1;
    else
        sidelen(1)=0;
    end

```

```

    end
    t=1;
%end
    for j=i:columns
        if seg_mask(rows,j)~=0

            shadow=2;

            xdown(t) = j;
            ydown(t) = rows;
            new = t;
            t=t+1;
        end

    end

    if(shadow==2)

        sidelen(2) = t-1;
    end
    if(shadow~=2 && shadow>0)
        sidelen(2)=0;
    end
    t=1;
    for j=i:columns
        if seg_mask(i,j)~=0

            shadow=3;
            xup(t) = j;
            yup(t)=i;
            t=t+1;
        end
    end
    if(shadow==3)
        sidelen(3) = t-1;

    end

    if(shadow~=3 && shadow>0)
        sidelen(3)=0;
    end
end

```

```

t=1;

for j=i:rows
if seg_mask(j,i)~=0

    shadow=4;
    xleft(t)=i;
    yleft(t)=j;
    t=t+1;
end
end

if(shadow==4)
sidelen(4) = t-1;
if(shadow~=4 && shadow>0)
sidelen(4)=0;
end

end

```

%%%%%%%%% If the shadow region touched two or more sides, it takes the side with the most coverage %%%%%%%%%%

```

maxside = max(sidelen);
side = find(sidelen==maxside);
if(side==1)
    xaxis=[];
    yaxis=[];
    for i=1:length(yright)

        xaxis(i) = xright(i);
        yaxis(i) = yright(i);

    end
end

if(side==2)
    xaxis=[];
    yaxis=[];
    for i=1:length(xdown)

```

```
xaxis(i) = xdown(i);
yaxis(i) = ydown(i);
```

```
end
end
```

```
if(side==3)
xaxis=[];
yaxis=[];
for i=1:length(xup)
xaxis(i) = xup(i);
yaxis(i) = yup(i);
```

```
end
end
```

```
if(side==4)
xaxis=[];
yaxis=[];
for i=1:length(yleft)
xaxis(i) = xleft(i);
yaxis(i) = yleft(i);
```

```
end
end
```

```
%%%%%%%%%%%%% Applying Active Contour to the original image with finalmask as
ROI %%%%%%%%%%%%%%
img2=activecontour(img,finalmask,iteration,'Chan-Vese');
```

```
%%%%%%%%% shadow>0 means there is shadow in the image, so it applies Seed Region Growing Method to
eliminate shadow %%%%%%%%%%
```

```
if(shadow>0)
% Display the original gray scale image.
for n=1:length(xaxis)
row = yaxis(n);
column = xaxis(n);
```

```
%%%%%%%%%5 Get the gray level of the point they clicked on. %%%%%%%%%%
gray_lev = gray(row, column);
tol = 10;
```



```

% Construct abinary image within the gray level tolerance
% of where they clicked.
Gray_lev_low = gray_lev - tol;
Gray_lev_high = gray_lev + tol;
binaryImage = gray >= Gray_lev_low & gray <= Gray_lev_high;

finalwhite(n) = sum(binaryImage(:));
img_title = sprintf('Binary Image');
title(img_title);

%%%%%%%%%% Get a marker image to reconstruct just the connected region and not all the other
disconnected regions. %%%%%%%%%%
binMarkerImg = false(rows, columns);
binMarkerImg(row, column) = true;
binMarkerImg = im2bw(binMarkerImg,thresh(k));
resultImg = imreconstruct(binMarkerImg, binaryImage);

%%%%%%%%%% Get the masked image - the original image in the
region. %%%%%%%%%%
maskedImage = zeros(rows, columns, 'uint8');
maskedImage(resultImg) = gray(resultImg);
end

%%%%%%%%% for the ideal shadow cropping we set out condition %%%%%%%%%%5
minwhite = min(finalwhite);
[val,idx] = min(abs(finalwhite-mean(finalwhite)));
ind = min(idx);

%%%%%%%%% Find out the exact pixel for which the shadow cropping is ideal and applying Seed Region
Growing Method again. %%%%%%%%%%
row = yaxis(ind);
column = xaxis(ind);

gray_lev = gray(row, column);
tol = 10;
Gray_lev_low = gray_lev - tol;
Gray_lev_high = gray_lev + tol;
binaryImage = gray >= Gray_lev_low & gray <= Gray_lev_high;

%%%%%%%%% Show subplots for images with shadows %%%%%%%%%%5

```

```

figure(k)
p = uipanel('Parent',figure(k),'BorderType','none');
str = sprintf('Optimum Threshold Value: %.2f,thresh(k));
p.Title = (str);
p.TitlePosition = 'centertop';
p.FontSize = 12;
p.FontWeight = 'bold';
subplot(3,3,1,'Parent',p)
imshow( img, []);
title(sprintf('%s', imageName))
binMarkerImg = false(rows, columns);
binMarkerImg(row, column) = true;
resultImg = imreconstruct(binMarkerImg, binaryImage);
img3=activecontour(img,resultImg,iteration,'Chan-Vese');
mask1 = img3;

%%%%% Applying the shadow as white layer in the original image %%%%%%%%%%
maskedimage = imoverlay(img,img3,'white');

[rows, columns, number] = size(maskedimage);
if number > 1
maskedimage = rgb2gray(maskedimage);
end

finalmask = imoverlay(seg_mask,img3,'white');
finalmask=imcomplement(finalmask);
finalmask = im2bw(finalmask,thresh(k));

%%%%%%%%% making the white layered imahe black and white %%%%%%%%%%
bwx = im2bw(maskedimage,thresh(k));
minimum=0;
iteration=50;
thres=0;
s=1;
w=1;

%%%%%%%%% Applying Watershed Method for the shadow cropped image %%%%%%%%%%5
for q=0.1:0.01:0.5
bnw=im2bw(maskedimage,q);
inv_bnw= ~bnw;
C= -bwdist(inv_bnw);

```

```

C(inv_bnw)=-Inf;
M= watershed(C);
Wi= label2rgb(M,'jet','c');%for purpose of visualizing label region.
% The section below works as to measure, segment and segregate the Image in
% order to obtain the desired output.
img_label=bwlabel(M);
stats=regionprops(img_label,'Solidity','Area'); % returns measurements for the
% set of properties specified by properties for each 8-connected component (object) in the binary

% since the solidity of the tumor is greater than the breast solidity,
dens=[stats.Solidity];
img_area=[stats.Area];
high_dense_area=dens>0.5; %which means the area that has 50% Solidity than the breast is needed
maximum_area=max(img_area(high_dense_area)); %returns maximum area
tumor_label=find(img_area==maximum_area);
seg_tumor=ismember(img_label,tumor_label);%returns an array containing logical 1 (true).
%Elsewhere, the array contains logical 0 (false)
se=strel('square',5); %essential for dilation
seg_tumor=imdilate(seg_tumor,se); %for dilation i.e. making sure the tumor is filled with same value like
% The section below is Subplot which displays the results in and organize
% manner.
[B,M]=bwboundaries(seg_tumor,'noholes'); %draw boundaries around the tumor and no holes needed.

%% Determining Boundary of Tumor
for i=1:length(B)
[rows, columns, numberOfColorChannels] = size(maskedimage);
seg_mask = poly2mask(B{i}(:,2),B{i}(:,1), rows, columns);
end
Boundary = B{1}; % Whatever boundary you want.
x = Boundary(:, 2);
y = Boundary(:, 1);
yellowMask = poly2mask(x, y, rows, columns);
pixelsInyellowMask = bnw(yellowMask);
numBlack = sum(pixelsInyellowMask == 0)
numWhite = sum(pixelsInyellowMask == 1)
%% Placing The Selected Tumor in a White Background
value(s)=q;

%% Setting the Condition to Select The Optimum Threshold Value
if(numBlack>numWhite)
possibleOutput(w)=q;
w=w+1;

```

```

end
s=s+1;
    end
minimum=min(possibleOutput);
loc=find(value==minimum);
thresh(k)=value(loc);
bnw=im2bw(maskedimage,thresh(k));
    inv_bnw= ~bnw;
    C= -bwdist(inv_bnw);
    C(inv_bnw)= -Inf;
    M= watershed(C);
    Wi= label2rgb(M,'jet','c');%for purpose of visualizing label region.
    % The section below works as to measure, segment and segregate the Image in
% order to obtain the desired output.
img_label=bwlabel(M);
stats=regionprops(img_label,'Solidity','Area'); % returns measurements for the
% set of properties specified by properties for each 8-connected component (object) in the binary

% since the solidity of the tumor is greater than the breast solidity,
dens=[stats.Solidity];
img_area=[stats.Area];
high_dense_area=dens>0.5; %which means the area that has 50% Solidity than the breast is needed
maximum_area=max(img_area(high_dense_area)); %returns maximum area
tumor_label=find(img_area==maximum_area);
seg_tumor=ismember(img_label,tumor_label);%returns an array containing logical 1 (true).
%Elsewhere, the array contains logical 0 (false)
se=strel('square',5); %essential for dilation
seg_tumor=imdilate(seg_tumor,se); %for dilation i.e. making sure the tumor is filled with same value like

% The section below is Subplot which displays the results in and organize
% manner.
[B,M]=bwboundaries(seg_tumor,'noholes'); %draw boundaries around the tumor and no holes needed.
%imshow(img);
%hold on
for i=1:length(B)
    [rows, columns, numberOfColorChannels] = size(maskedimage);
    %plot(B{i}(:,2),B{i}(:,1), 'y', 'linewidth',1.45);
    seg_mask = poly2mask(B{i}(:,2),B{i}(:,1), rows, columns);
end

bw1=activecontour(bwx, finalmask, iteration,'Chan-Vese');

```

```

subplot(3,3,2)
imshow(maskedimage);
title("Eliminating Shadow Region", 'r');
subplot(3,3,3)
imshow(img);
hold on
for i=1:length(B)
    plot(B{i}(:,2),B{i}(:,1), 'r', 'linewidth',1.45);

end
title('Segmented Tumor');
hold off;

subplot(3,3,4)
imshow(img);
hold on
for i=1:length(B)
    plot(B{i}(:,2),B{i}(:,1), 'r', 'linewidth',1.45);
    seg_mask = poly2mask(B{i}(:,2),B{i}(:,1), rows, columns);

end
title('Segmented Tumor');
hold off;

subplot(3,3,4)
imshow(maskimage);
title("Reference");

subplot(3,3,6)
imshow(seg_mask);
title("Output Mask");

%%%%%%%%%% Result for different precision metrics %%%%%%%%%%%
subplot(3,3,7)
similarity = dice(seg_mask, maskimage);
imshowpair(seg_mask,maskimage);
title(['Dice Index = ' num2str(similarity)]);

subplot(3,3,8)
bf_sc = bfscore(finalmask, maskimage);
imshowpair(seg_mask, maskimage);
title(['BF Score = ' num2str(bf_sc)])

```

```

subplot(3,3,9)
jac = jaccard(finalmask, maskimage);
imshowpair(seg_mask, maskimage);
title(['Jaccard Index = ' num2str(jac)])
end
value=[];

%%%%% If the image has no shadow, we don't apply Seed Region Growing Method %%%%%%%%%%

if(shadow==0)
    figure(k)
    p = uipanel('Parent',figure(k),'BorderType','none');

    str = sprintf('Optimum Threshold Value: %.2f',thresh(k));

    p.Title = (str);
    p.TitlePosition = 'centertop';
    p.FontSize = 12;
    p.FontWeight = 'bold';
    subplot(3,3,1,'Parent',p)
    imshow(img);
    %title('Image')
    title(sprintf('%s', imageName))

    subplot(3,3,3,'Parent',p)
    %bw2 = medfilt2(bw1,[2 2]);

    imshow(img)
    if(shadow==1)
        shadowtitle="Shadow Detected";
    end
    if(shadow==0)
        shadowtitle="No Shadow Detected";
    end
    title(shadowtitle,'Color','b')
    hold on
    h = visboundaries(img2,'Color','r');

    h.Children(1);
    h.Children(2);
    h.Children(2).Visible = 'off';

```

```

h.Children(1).LineWidth = 1;

subplot(3,3,4)
imshow(maskimage);
title("Reference");

subplot(3,3,6)
imshow(finalmask);
title("Output Mask");

%%%%%%%%%% Result for different precision metrics %%%%%%%%%%%
subplot(3,3,7)
similarity = dice(finalmask, maskimage);
imshowpair(finalmask,maskimage);
title(['Dice Index = ' num2str(similarity)]);

subplot(3,3,8)
bf_sc = bfscore(finalmask, maskimage);
imshowpair(finalmask, maskimage);
title(['BF Score = ' num2str(bf_sc)])

subplot(3,3,9)
jac = jaccard(finalmask, maskimage);
imshowpair(finalmask, maskimage);
title(['Jaccard Index = ' num2str(jac)])
end
    end
end

```